NPS67-88-002CR

NAVAL POSTGRADUATE SCHOOL
Monterey, California

CONTRACTOR REPORT

FAR FIELD NUMERICAL BOUNDARY CONDITIONS

FOR INTERNAL AND CASCADE FLOW COMPUTATIONS

CHARLES HIRSCH
VRIJE UNIVERSITEIT BRUSSEL
PLEINLANN 2
1050 BRUSSEL, BELGIUM

NOVEMBER 1988

APPROVED FOR PUBLIC RELEASE; DISTRIBUTION UNLIMITED.

PREPARED FOR: NAVAL POSTGRADUATE SCHOOL
MONTEREY, CALIFORNIA 93943-5000

90 01 11 113

NAVAL POSTGRADUATE SCHOOL
Monterey, California

RADM R. W. West, JR.   H. SHULL
Superintendent   Provost

The present study was performed under contract N62271-87-M-0215 during the period June-November 1988. The author previously served as the Naval Air Systems Command Research Professor in Aeronautics during FY84. The prior appointment and the present study were sponsored by the Air-Breathing Propulsion Research Program at NAVAIR under the cognizance of G. Derderian (AIR 931E).
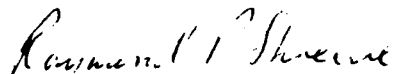
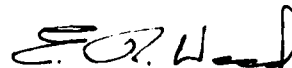This report was prepared by:

_____
Ch. Hirsch

Publication of the report does not constitute approval of the sponsor for the findings or conclusions. It is published for information and for the exchange and stimulation of ideas.
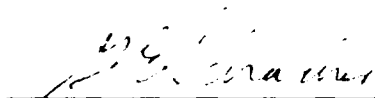

Reviewed by:

_____   _____
RAYMOND P. SHREEVE   E. R. WOOD
Professor   Chairman
Department of Aeronautics   Department of Aeronautics
      and Astronautics   and Astronautics

Released by:

_____
G. E. SCHACHER
Dean of Science and Engineering

REPORT DOCUMENTATION PAGE

1a. REPORT SECURITY CLASSIFICATION UNCLASSIFIED		1b RESTRICTIVE MARKINGS			
2a. SECURITY CLASSIFICATION AUTHORITY		3 DISTRIBUTION/AVAILABILITY OF REPORT APPROVED FOR PUBLIC RELEASE: DISTRIBUTION IS UNLIMITED			
2b. DECLASSIFICATION/DOWNGRADING SCHEDULE					
4. PERFORMING ORGANIZATION REPORT NUMBER(S) NPS67-88-002CR		5 MONITORING ORGANIZATION REPORT NUMBER(S) NPS67-88-002CR			
6a. NAME OF PERFORMING ORGANIZATION PROF. DR. IR. CHARLES HIRSCH VRIJE UNIVERSITEIT, BRUSSEL	6b OFFICE SYMBOL (If applicable)	7a. NAME OF MONITORING ORGANIZATION NAVAL POSTGRADUATE SCHOOL			
6c. ADDRESS (City, State, and ZIP Code) PLEINLAAN 2 1050 BRUSSELS, BELGIUM		7b. ADDRESS (City, State, and ZIP Code) MONTEREY, CALIFORNIA 93943-5000			
8a. NAME OF FUNDING/SPONSORING ORGANIZATION NAVAL AIR SYSTEMS COMMAND	8b OFFICE SYMBOL (If applicable) AIR931E	9. PROCUREMENT INSTRUMENT IDENTIFICATION NUMBER N62271-87-M-0215			
8c. ADDRESS (City, State, and ZIP Code) WASHINGTON, D.C. 20361		10 SOURCE OF FUNDING NUMBERS			
		PROGRAM ELEMENT NO. 61153N	PROJECT NO WR024	TASK NO 03	WORK UNIT ACCESSION NO. 001

11. TITLE (Include Security Classification)

FAR FIELD NUMERICAL BOUNDARY CONDITIONS FOR INTERNAL AND CASCADE FLOW COMPUTATIONS

12. PERSONAL AUTHOR(S)
HIRSCH, CHARLES

13a. TYPE OF REPORT FINAL	13b TIME COVERED FROM 6/88 TO 9/88	14 DATE OF REPORT (Year, Month, Day) 1988, NOVEMBER	15 PAGE COUNT 54

16. SUPPLEMENTARY NOTATION

17. COSATI CODES			18 SUBJECT TERMS (Continue on reverse if necessary and identify by block number)
FIELD	GROUP	SUB-GROUP	COMPUTATIONAL BOUNDARY CONDITIONS INTERNAL FLOW COMPUTATIONS CASCADE FLOW COMPUTATIONS

19 ABSTRACT (Continue on reverse if necessary and identify by block number)

The present report extends the approach developed by A. Verhoff for the treatment of the far field boundary conditions, Verhoff and O'Neil (1984), to more general formulations of the Euler equations and to cascade geometries. Linearized solutions of the Euler equations are developed for the perturbations from the uniform free stream, for ducts and cascades. These solutions are based on the conditions that the waves associated with incoming characteristic should decay to zero in the far field, while the variables associated to the outgoing characteristics are derived from the numerical internal solution. The exact linearized solutions are based on a Fourier expansion in the direction along the inlet or exit boundaries. Result obtained from an Euler code are shown for ducts and cascades, comparing calculations for exit boundaries at increasingly closer distance to the central flow region. The method is also valid for nonisentropic flows. The results show that the corrections to the uniform boundary conditions derived from the analysis allow a considerable reduction of the computational domain, with the corresponding savings in computational times.

20 DISTRIBUTION/AVAILABILITY OF ABSTRACT ☒ UNCLASSIFIED/UNLIMITED ☐ SAME AS RPT ☐ DTIC USERS	21 ABSTRACT SECURITY CLASSIFICATION UNCLASSIFIED	
22a NAME OF RESPONSIBLE INDIVIDUAL R. P. SHREEVE	22b TELEPHONE (Include Area Code) (408) 646-2593	22c OFFICE SYMBOL 67Sf

DD FORM 1473, 84 MAR — 83 APR edition may be used until exhausted — SECURITY CLASSIFICATION OF THIS PAGE
All other editions are obsolete

☆ U.S. Government Printing Office 1986—606-2

FAR FIELD NUMERICAL BOUNDARY CONDITIONS FOR INTERNAL AND CASCADE FLOW COMPUTATIONS

Ch. HIRSCH,
Department of Fluid Mechanics,
Vrije Universiteit Brussel, Belgium

NOVEMBER 1988

LIST OF FIGURES

NOMENCLATURE

b	channel width
c	speed of sound
c_p	specific heat under constant pressure
f,g,h	Fourier coefficients of characteristic perturbations
h	enthalpy
H	stagnation enthalpy
$\hat{i}$	unit vector perpendicular to the wave propagation direction
M	Mach number
n	direction normal to velocity
p	pressure
q	velocity amplitude
r	gas constant per unit mass
s	cascade pitch
s	entropy
S	dimenlionless entropy (equation 1.3a)
u	x-component of velocity
y	time
v	y-component of velocity
$\vec{v}$	velocity vector
w_i	i=1 to 4, characteristic variables
x,y	cartesian coordinates

α	angle of wave propagation direction
β	$\beta^2 = 1 - M_\infty^2$
γ	specific heat ratio
$\vec{\kappa}$	wave propagation vector (unit vector)
μ	coefficient for streamwise exponential variation of wave disturbances
ϕ	phase angle of Fourier mode (equation 3.4)
ρ	density
ω	vorticity
θ	flow angle
τ	transformed time variable (equation 1.22)

Subscripts

0	boundary values
∞	free stream values

Superscripts

'	perturbations of corresponding quantity

FAR FIELD NUMERICAL BOUNDARY CONDITIONS FOR INTERNAL AND CASCADE FLOW COMPUTATIONS

Ch. HIRSCH,
Department of Fluid Mechanics,
Vrije Universiteit Brussel, Belgium

ABSTRACT

The present report extends the approach developed by A. Verhoff for the treatment of the far field boundary conditions, Verhoff and O'Neil (1984), to more general formulations of the Euler equations and to cascade geometries.

Linearized solutions of the Euler equations are developed for the perturbations from the uniform free stream, for ducts and cascades. These solutions are based on the conditions that the waves associated with incoming characteristics should decay to zero in the far field, while the variables associated to the outgoing characteristics are derived from the numerical internal solution. The exact linearized solutions are based on a Fourier expansion in the direction along the inlet or exit boundaries.

Results, obtained from an Euler code are shown for ducts and cascades, comparing calcualtions for exit boundaries at increasingly closer distance to the central flow region. The method is also valid for nonisentropic flows.

The results show that the corrections to the uniform boundary conditions derived from the analysis allow a considerable reduction of the computational domain, with the corresponding savings in computational times.

FAR FIELD NUMERICAL BOUNDARY CONDITIONS FOR INTERNAL AND CASCADE FLOW COMPUTATIONS

Ch. HIRSCH,
Department of Fluid Mechanics,
Vrije Universiteit Brussel, Belgium

INTRODUCTION

The present report extends the approach developed by A. Verhoff for the treatment of the far field boundary conditions, Verhoff and O'Neil, (1984), Verhoff (1988), to more general formulations of the Euler equations and to cascade geometries.

The imposition of uniform boundary conditions in the subsonic far field of the computational domain, such as constant pressure condition, requires the computational boundary to be located at a large distance from the central flow region. Although the flow variations in the vicinity of the external boundaries are generally smooth, a large number of mesh point are necessary to cover adequately these extended regions.

If more information would be available on the behavior of the flow in the far field, allowing for non-uniform flow distributions along boundaries, it would be possible to accept external boundaries at distances much closer to the main flow region, with the subsequent reduction in number of mesh points.

In this report linearized solutions of the Euler equations are developed for the perturbations from the uniform free stream, for ducts and cascades. These solutions are based on the conditions that the waves associated with incoming characteristics should decay to zero in the far field, while the variables associated to the outgoing characteristics are derived from the numerical internal solution. The exact linearized solutions are based on a Fourier expansion in the direction along the inlet or exit boundaries.

Typical outcome of the analysis leads, for a cascade exit station with subsonic axial velocities, to the replacement of the constant pressure condition by an improved boundary condition, relating the pressure perturbations to the Fourier expansion of the flow angle along the exit boundary calculated from the numerical internal solution.

Results are also presented for ducts and cascades, comparing the results for exit boundaries at increasingly closer distance to the cascade blades.

In the first part, sections 1 and 2, we present a reformulation of A. Verhoff's (1985) isentropic analysis for ducts, based on the perturbation analysis of the general form of the characteristic equations, as applied by Hirsch et al.(1987). The first order equations are identical to those derived by Verhoff for his generalized Riemann invariants, although the acoustic wave perturbations are represented by a different combination of variables. This covers therefore isentropic as well as non-isentropic flows. As a by-product, an interesting relation is derived, relating the far field pressure and velocity fluctuations for isentropic flows.

The third section presents the extension of the approach to cascades. Due to the periodicity boundary conditions in the inlet and outlet domains, resp. upstream and downstream of the cascade blades, a complex Fourier representation has to be defined for the variations in the direction of the cascade front. Results, obtained from an Euler code are shown for ducts and cascades, confirming the correctness of the analysis and the potential CPU benefits of closer boundaries.

1.PERTURBATION ANALYSIS FOR GENERALIZED CHARACTERISTIC EQUATIONS.

The small perturbation formulation of the Euler equations can be derived in many ways, depending on the particular variables considered for the analysis. The most current

formulation puts forward the pressure, since it is the basis for all acoustic applications, and takes the Euler equations in primitive variables, p,ρ and velocity, as starting point.

In computational fluid dynamics, appropriate information on outgoing pressure radiation waves allows to investigate far field boundary conditions, which should prevent spurious waves to be reflected from the boundaries towards the computational domain. This has been investigated by Bayliss and Turkel (1982), where references can also be found to earlier important work in that direction and more recently by P.Roe (1986). In these methods, differential equations for the pressure are derived for the far field pressure and added, after appropriate discretization, to the other internal equations.

Other approaches make use of the far field formulation of the small perturbation potential equation and introduce analytical asymptotic expansions as boundary corrections, Thomas and Salas (1986).

In the present approach, numerical information is used directly in interaction with a series expansion of the far field, applying a perturbation expansion of the characteristic equations. Hence, we take as starting point, the compatibility equations. Note that these different point of views are clearly interconnected: Roe (1986) derives a particular form of the acoustic compatibility equation corresponding to a selected wave propagation direction which corresponds to the selected pressure equation. In the present work, far-field pressure relations will be derived from the characteristic analysis.

1.1. Euler equations in characteristic form

We consider the general form of the Euler equations in characteristic form, written for an arbitrary direction of wave propagation $\vec{\kappa}$, considered as a unit vector, following Hirsch et al. (1987), see also Hirsch (1988), (1989).

The dependent variables are the following characteristic quantities, defined in differential form,

$$\partial w_1 = \partial \rho - \frac{1}{c^2}\partial p \tag{1.1a}$$

$$\partial w_2 = \vec{l}.\partial \vec{v} = \kappa_y \partial u - \kappa_x \partial v \tag{1.1b}$$

$$\partial w_3 = \vec{\kappa}.\partial \vec{v} + \frac{1}{\rho c}\partial p = \kappa_x \partial u + \kappa_y \partial v + \frac{1}{\rho c}\partial p \tag{1.1c}$$

$$\partial w_4 = - \vec{\kappa}.\partial \vec{v} + \frac{1}{\rho c}\partial p = - (\kappa_x \partial u + \kappa_y \partial v) + \frac{1}{\rho c}\partial p \tag{1.1d}$$

where the vector $\vec{l}$ is normal to the wave number vector $\vec{\kappa}$ and has the components $(\kappa_y, - \kappa_x)$. Note that $\vec{l}$ is also a unit vector; see figure 1.1.

The first characteristic variable is proportional to the entropy and the associated equation will describe the convection (propagation) of entropy (waves). The second component is the amplitude of a vorticity or shear wave, which has no equivalent in one dimensional flows. The third and fourth components are the amplitudes of the acoustic waves.

The compatibility equations for the Euler system of conservation laws, become

$$\partial_t w_1 + (\vec{v}.\vec{\nabla})w_1 = 0 \tag{1.2a}$$

$$\partial_t w_2 + (\bar{v}.\bar{\nabla})w_2 + \frac{c}{2}(\hat{l}.\bar{\nabla})(w_3 + w_4) = 0 \qquad (1.2b)$$

$$\partial_t w_3 + (\bar{v} + c\vec{\kappa}).\bar{\nabla}w_3 + c(\hat{l}.\bar{\nabla})w_2 = 0 \qquad (1.2c)$$

$$\partial_t w_4 + (\bar{v} - c\vec{\kappa}).\bar{\nabla}w_4 + c(\hat{l}.\bar{\nabla})w_2 = 0 \qquad (1.2d)$$

The first two terms of all the equations (1.2) are purely convective and represent the propagation of the associated wave in the characteristic directions. The third terms represent the coupling or the interaction between the different waves and their presence results from the fact that the jacobian matrices are not simultaneously diagonalizable for wave-like solutions of the form $U = U_0 e^{-i\vec{\kappa}.\bar{x}} e^{i\omega t}$ whereby all the components of U, that is all the flow variables, propagate along the same spatial direction $\vec{\kappa}$.

If this direction is taken aligned with the velocity, than the above equations can be transformed to the particular streamwise characteristic form used by Verhoff, Verhoff and O'Neil(1984). Defining the dimensionless entropy as

$$S = -s/(\gamma r) \qquad (1.3a)$$

where s is the physical entropy and r the gas constant, we have

$$S - S_\infty = \frac{-1}{\gamma(\gamma-1)} \log\left[\frac{p/p_\infty}{\left(\rho/\rho_\infty\right)^\gamma}\right] \qquad (1.3b)$$

with

$$dS = \frac{1}{\rho(\gamma-1)} dw_1 \qquad (1.3c)$$

The constant S_∞ is taken as $S_\infty = 2/(\gamma-1)$.

Hence, the first characteristic equation reduces to the convection of entropy,

$$\frac{\partial S}{\partial t} + q\frac{\partial S}{\partial s} = 0 \qquad (1.4)$$

where ds is the elementary arc length along the flow pathline and q the magnitude of the velocity.

The second characteristic variable

$$\partial w_2 = \hat{l}.\partial\bar{v} \qquad (1.5)$$

reduces to the following form for a direction $\vec{\kappa} = \vec{1}_v$, the unit vector in the direction of the velocity and $\hat{l} = \vec{1}_n$ the unit vector in the direction normal to the velocity, figure 1.2. With

$$d\bar{v} = dq\vec{1}_v + qd\theta\vec{1}_n \qquad (1.6)$$

$$\partial w_2 = \vec{1}_v \cdot \partial \vec{v} \tag{1.7}$$

the second equation (1.2b) becomes

$$\frac{\partial \theta}{\partial t} + (\vec{v} \cdot \vec{\nabla})\theta + \frac{c^2}{\gamma q}\frac{\partial P}{\partial n} = 0 \tag{1.8}$$

where P is the logarithm of the pressure and $\partial/\partial n$ is the derivative in the direction normal to the velocity.

The third characteristic variable is written in the following form

$$\partial w_3 = \frac{\partial p}{\rho c} + \vec{1}_v \cdot \partial \vec{v} = \frac{\partial p}{\rho c} + \partial q \tag{1.9}$$

and equation (1.2c) becomes

$$\frac{\partial w_3}{\partial t} + (q+c)\frac{\partial w_3}{\partial s} + qc\frac{\partial \theta}{\partial n} = 0 \tag{1.10}$$

Introducing equation (1.9) and expressing the pressure variations dp in function of the variations of entropy and speed of sound, via the definition $c^2 = \gamma p/\rho$ for a perfect gas and equation (1.3), leads to

$$\frac{dp}{\rho c} = cdS + \frac{2}{\gamma-1}dc = d(cS) - (S - \frac{2}{\gamma-1})dc \tag{1.11}$$

The formulation of the Euler equations used by Verhoff is based on 'generalized' Riemann variables R and Q, defined as R=q-cS and Q=q+cS and equation (1.10) can be transformed to

$$\frac{\partial(q+cS)}{\partial t} + (q+c)\frac{\partial(q+cS)}{\partial s} = (S - \frac{2}{\gamma-1})[\frac{\partial c}{\partial t} + (q+c)\frac{\partial c}{\partial s}] - qc\frac{\partial \theta}{\partial n} \tag{1.12}$$

Note also the interesting relation for the speed of sound

$$\frac{\partial c}{\partial t} + q\frac{\partial c}{\partial s} = -\frac{\gamma-1}{2}c(\vec{\nabla} \cdot \vec{v}) \tag{1.13}$$

and with the expression of the divergence of the velocity in local coordinates,

$$\vec{\nabla} \cdot \vec{v} = \frac{\partial q}{\partial s} + q\frac{\partial \theta}{\partial n} \tag{1.14}$$

equation (1.12) reduces to the form

$$\frac{\partial(q+cS)}{\partial t} + (q+c)\frac{\partial(q+cS)}{\partial s} = (S - \frac{2}{\gamma-1}) c (\frac{\partial c}{\partial s} - \frac{\gamma-1}{2}\frac{\partial q}{\partial s}) - \frac{\gamma-1}{2}qcS\frac{\partial \theta}{\partial n} \tag{1.15}$$

used by Verhoff and O'Neil(1984).
The fourth characteristic equation leads to the similar equation for the variable R=q-cS

$$\frac{\partial(q\text{-}cS)}{\partial t} + (q\text{-}c)\frac{\partial(q\text{-}cS)}{\partial s} = (S - \frac{2}{\gamma\text{-}1})\,c\,(\frac{\partial c}{\partial s} + \frac{\gamma\text{-}1}{2}\frac{\partial q}{\partial s}) + \frac{\gamma\text{-}1}{2}qcS\frac{\partial\theta}{\partial n} \qquad (1.16)$$

Equations (1.4), (1.8), (1.15) and (1.16) are identical to the 'Quasi 1D' formulation of Verhoff and
O'Neil (1984).

1.2. Perturbation expansion in the far field

If the flow at infinity is uniform, at any finite distance a perturbation will exist, which is supposed to be small at some distance from the central region of the flow domain. Denoting by a subscript ∞ the uniform quantities and writing all variables U as $U=U_\infty+\varepsilon U'$, where ε is a small perturbation parameter, the first order linearized Euler equations (1.2) take the form

$$\partial_t w'_1 + (\vec{V}_\infty.\vec{\nabla})w'_1 = 0 \qquad (1.17a)$$

$$\partial_t w'_2 + (\vec{V}_\infty.\vec{\nabla})w'_2 + \frac{1}{\rho_-}\,(\vec{l}.\vec{\nabla})p' = 0 \qquad (1.17b)$$

$$\partial_t w'_3 + (\vec{V}_\infty + c_\infty\vec{\kappa}).\vec{\nabla}w'_3 + c_\infty(\vec{l}.\vec{\nabla})w'_2 = 0 \qquad (1.17c)$$

$$\partial_t w'_4 + (\vec{V}_\infty - c_\infty\vec{\kappa}).\vec{\nabla}w'_4 + c_\infty(\vec{l}.\vec{\nabla})w'_2 = 0 \qquad (1.17d)$$

The perturbation equations are written here in the general form for an arbitrary wave propagation direction and the first order corrections w' of the characteristic variables are defined as follows, in function of the perturbations S', p' and $\vec{v}'$ of resp. entropy, pressure and velocity. The first characteristic variable w'_1 is proportional to the entropy, hence we have, following equation (1.3b),

$$w'_1 = \rho(\gamma\text{-}1)S' \qquad (1.18)$$

while the second characteristic variable w'_2, in accordance with equation (1.5), is defined as

$$w'_2 = \vec{l}.\vec{v}' = v'\cos\alpha - u'\sin\alpha \qquad (1.19a)$$

referring to figure 1.3, α being the angle betwen the propagation direction $\vec{\kappa}$ and the reference x-direction and u', v' the cartesian components of the perturbation velocity. In function of the flow angle deviation θ' to the free stream angle θ_∞, and the projection q'

of the velocity perturbation on the direction of the far field velocity, the above equation can also be written as

$$w_2' = q_\infty \theta' \cos(\alpha - \theta_\infty) - q' \sin(\alpha - \theta_\infty) \qquad (1.19b)$$

The perturbations of the third and fourth characteristic variables are defined by

$$w_3' = \frac{p'}{\rho_\infty c_\infty} + q_\infty \theta' \sin(\alpha - \theta_\infty) + q' \cos(\alpha - \theta_\infty) \qquad (1.20)$$

$$w_4' = \frac{p'}{\rho_\infty c_\infty} - q_\infty \theta' \sin(\alpha - \theta_\infty) - q' \cos(\alpha - \theta_\infty) \qquad (1.21)$$

Transforming the time variable to a variable with space dimensions, via

$$\tau = c_\infty t \qquad (1.22)$$

and introducing the free stream Mach number

$$M_\infty = q_\infty/c_\infty \qquad (1.23)$$

leads to the following form of the first order perturbation equations, where x and y are reference cartesian coordinates.

$$\frac{\partial S'}{\partial \tau} + M_\infty (\cos\theta_\infty \frac{\partial}{\partial x} + \sin\theta_\infty \frac{\partial}{\partial y}) S' = 0 \qquad (1.24a)$$

$$\frac{\partial w_2'}{\partial \tau} + M_\infty (\cos\theta_\infty \frac{\partial}{\partial x} + \sin\theta_\infty \frac{\partial}{\partial y}) w_2' - \frac{1}{2} (\sin\alpha \frac{\partial}{\partial x} - \cos\alpha \frac{\partial}{\partial y})(w_3' + w_4') = 0 \qquad (1.24b)$$

$$\frac{\partial w_3'}{\partial \tau} + (M_\infty \cos\theta_\infty + \cos\alpha) \frac{\partial w_3'}{\partial x} + (M_\infty \sin\theta_\infty + \sin\alpha) \frac{\partial w_3'}{\partial y} - \sin\alpha \frac{\partial w_2'}{\partial x} + \cos\alpha \frac{\partial w_2'}{\partial y} = 0 \qquad (1.24c)$$

$$\frac{\partial w_4'}{\partial \tau} + (M_\infty \cos\theta_\infty - \cos\alpha) \frac{\partial w_4'}{\partial x} + (M_\infty \sin\theta_\infty - \sin\alpha) \frac{\partial w_4'}{\partial y} - \sin\alpha \frac{\partial w_2'}{\partial x} + \cos\alpha \frac{\partial w_2'}{\partial y} = 0 \qquad (1.24d)$$

Note that the average of the acoustic wave perturbations is proportional to the pressure disturbance p'

$$(w_3' + w_4')/2 = \frac{p'}{\rho_\infty c_\infty} \qquad (1.25)$$

and that the second equation (1.24b) relates the flow angle perturbations θ' to the far field pressure disturbance.

1.2.1. Simplified formulation

7

A simplified form is obtained when the wave propagation direction $\vec{\kappa}$ is aligned with the free stream velocity direction, that is for $\alpha = \theta_\infty$. In addition, the x-direction can also be aligned with the free stream velocity, that is $\alpha = \theta_\infty = 0$ and the above equations simplify considerably.

The characteristic variables reduce to

$$w_1' = \rho(\gamma - 1)S' \tag{1.26a}$$

$$w_2' = q_\infty \theta' \tag{1.26b}$$

$$w_3' = \frac{p'}{\rho_\infty c_\infty} + u' \tag{1.26c}$$

$$w_4' = \frac{p'}{\rho_\infty c_\infty} - u' \tag{1.26d}$$

and the system (1.24) becomes

$$\frac{\partial S'}{\partial \tau} + M_\infty \frac{\partial S'}{\partial x} = 0 \tag{1.27a}$$

$$\frac{\partial w_2'}{\partial \tau} + M_\infty \frac{\partial w_2'}{\partial x} + \frac{1}{2}\frac{\partial(w_3' + w_4')}{\partial y} = 0 \tag{1.27b}$$

$$\frac{\partial w_3'}{\partial \tau} + (M_\infty + 1)\frac{\partial w_3'}{\partial x} + \frac{\partial w_2'}{\partial y} = 0 \tag{1.27c}$$

$$\frac{\partial w_4'}{\partial \tau} + (M_\infty - 1)\frac{\partial w_4'}{\partial x} + \frac{\partial w_2'}{\partial y} = 0 \tag{1.27d}$$

This formulation of the first order perturbation equations is identical to the isentropic formulation applied by Verhoff (1985).

1.2.2. Relation between pressure and velocity disturbances

An interesting relation connecting pressure, velocity and entropy disturbances can be obtained, to first order, from energy conservation or constancy of stagnation enthalpy.

Writing $h + q^2/2 = H_\infty$ and expanding to first order leads to the following relation between enthalpy and velocity perturbations

$$h' + q'q_\infty = 0 \tag{1.28}$$

where q' is the perturbation of the magnitude of the far field velocity. This quantity is not equal to the magnitude of the velocity disturbance $\vec{v}'$ and we have $q' \approx u'$.

Expanding the definition of enthalpy in function of entropy and pressure

$$\frac{h}{h_\infty} = \left(\frac{p}{p_\infty}\right)^{\frac{\gamma-1}{\gamma}} e^{\frac{s-s_\infty}{c_p}} \qquad (1.29)$$

leads to

$$\frac{h'}{h_\infty} = \frac{\gamma-1}{\gamma} \frac{p'}{p_\infty} + \frac{s'}{c_p} \qquad (1.30)$$

Combining with equation (1.28), we obtain with the perfect gas relation $h_\infty = c_\infty^2 /(\gamma-1)$ and the dimensionless entropy disturbance S',

$$\frac{p'}{\rho_\infty c_\infty} + q'M_\infty - c_\infty S' = 0 \qquad (1.31)$$

The interest of this relation is that it expresses the far field influences of entropy fluctuations on the relations between the velocity and pressure fluctuations.

The acoustic wave amplitudes dw_3 and dw_4 can also be expressed in function of entropy, speed of sound and velocity, after elimination of the pressure through the entropy relation (1.11), leading to

$$dw_3 = cdS + \frac{2}{\gamma-1} dc + dq \qquad (1.32)$$

if the wave propagation direction $\vec{\kappa}$ is aligned with the local velocity. Similarly,

$$dw_4 = cdS + \frac{2}{\gamma-1} dc - dq \qquad (1.33)$$

The perturbations of these quantities can readily be defined and also can be combined with equation (1.31), to give

$$w_3' = \frac{p'}{\rho_\infty c_\infty} + q' = c_\infty S' + \frac{2c'}{\gamma-1} + q'$$

$$= c_\infty S' + (1-M_\infty)q' \qquad (1.34)$$

and

$$w_4' = \frac{p'}{\rho_\infty c_\infty} - q' = c_\infty S' + \frac{2c'}{\gamma-1} - q'$$

$$= c_\infty S' - (1+M_\infty)q' \qquad (1.35)$$

These equations imply the following relation between velocity and speed of sound perturbations,

$$-M_\infty q' = \frac{2c'}{\gamma-1} \tag{1.36}$$

which is obtained from equation (1.28) by an expansion of the perfect gas relation

$$h = c^2/(\gamma-1) \tag{1.37}$$

writing
$$c = c_\infty + c' \tag{1.38}$$

2. FAR FIELD BOUNDARY CONDITIONS FOR INTERNAL DUCT FLOWS

The determination of far field boundary conditions, based on the expansion of the characteristics small perturbations, is described in this section for duct flows, with subsonic in- and outflow conditions.

The derivation follows the approach of Verhoff (1985) and is repeated here with the w' variables, leading to some interesting relations for the pressure and velocity corrections.

The method determines analytical, steady state solutions for the perturbation wave amplitudes with exponential decay in the streamwise direction (taken as the x-direction) and a Fourier expansion in the direction of the boundary surfaces (taken as the y-direction). The unknown coefficients of the solutions are determined, on one hand, by expressing that the incoming characteristic disturbances at the boundaries decay exponentially in the far field and on the other hand, by matching the analytical solution at the boundary of the computational domain with the numerical solution for the outgoing characteristics.

The analysis is performed for stationary flows, for the simplified formulation (1.27) and a duct geometry represented in figure 2.1.

The duct extends to infinity with a computational region limited by inlet and exit boundaries AB and CD, the width of the channel being denoted by b. We look for perturbation solutions of the system (1.27) **in the region between the inlet (or exit) station of the computational domain and the boundary at infinity.**

Since entropy is purely convected and decoupled from the other equations, we can solve separately for the entropy perturbation and remove the corresponding equation from the system (1.27).

Disturbance solutions by separation of variables are sought for the remaining variables in the external region, with a Fourier series in y, of the form

$$w'_2 = \sum_{m=1}^{\infty} h_m(x) \sin\frac{m\pi y}{b} \tag{2.1a}$$

$$w'_3 = \sum_{m=1}^{\infty} f_m(x) \cos\frac{m\pi y}{b} \tag{2.1b}$$

$$w'_4 = \sum_{m=1}^{\infty} g_m(x) \cos\frac{m\pi y}{b} \tag{2.1c}$$

The choice of the Fourier terms in equation (2.1a) results from the flow tangency boundary condition at the solid walls, requiring that $\theta'=0$ for $y = \pm b/2$. Introducing these solutions in the stationary form of equations (1.27) leads to the following system, for an arbitrary Fourier mode m, writing M instead of M_∞, and removing the subscript m on the amplitudes f, g and h.

$$(M+1)\frac{\partial f}{\partial x} + \frac{m\pi}{b} h = 0$$

$$(M-1)\frac{\partial g}{\partial x} + \frac{m\pi}{b} h = 0 \tag{2.2}$$

$$M\frac{\partial h}{\partial x} - \frac{m\pi}{2b} (f+g) = 0$$

Defining the vector U as

$$U = \begin{vmatrix} f \\ g \\ h \end{vmatrix} \tag{2.3}$$

the system (2.2) can be written in matrix form

$$U_x + A U = 0 \tag{2.4a}$$

where the subscript x denotes partial derivative with respect to x and where the matrix A is

$$A = \begin{vmatrix} 0 & 0 & \dfrac{m\pi}{b(M+1)} \\ 0 & 0 & \dfrac{m\pi}{b(M-1)} \\ \dfrac{-m\pi}{2Mb} & \dfrac{-m\pi}{2Mb} & 0 \end{vmatrix} \tag{2.4b}$$

Solutions of the form

$$U = U_0 e^{-\mu x} \tag{2.5}$$

exist for μ equal to the eigenvalues of A, obtained from the solutions of det $(A - \mu I) = 0$, leading to

$$\mu_1 = 0$$

$$\mu_{2,3} = \pm \frac{m\pi}{b\beta}$$

(2.6)

with $\beta^2 = 1 - M^2$.

The corresponding amplitudes are the eigenvectors of A, denoted by $U^{(i)}$, and are given by

$$U^{(1)} = \begin{vmatrix} 1 \\ -1 \\ 0 \end{vmatrix} \qquad U^{(2)} = \begin{vmatrix} \dfrac{\beta}{M+1} \\ \dfrac{-\beta}{1-M} \\ 1 \end{vmatrix} \qquad U^{(3)} = \begin{vmatrix} \dfrac{-\beta}{M+1} \\ \dfrac{\beta}{1-M} \\ 1 \end{vmatrix} \qquad (2.7)$$

Hence, the general solution is written as a linear combination of the above eigenvectors,

$$U = \sum_{i=1}^{3} C_i U^{(i)} e^{-\mu_i x}$$

(2.8)

or explicitly,

$$\begin{vmatrix} f \\ g \\ h \end{vmatrix} = C_1 \begin{vmatrix} 1 \\ -1 \\ 0 \end{vmatrix} + C_2 \begin{vmatrix} \dfrac{\beta}{M+1} \\ \dfrac{-\beta}{1-M} \\ 1 \end{vmatrix} e^{-\frac{m\pi}{b\beta}x} + C_3 \begin{vmatrix} \dfrac{-\beta}{M+1} \\ \dfrac{\beta}{1-M} \\ 1 \end{vmatrix} e^{\frac{m\pi}{b\beta}x} \qquad (2.9)$$

The C-coefficients are determined by matching these solutions with the **numerical solution** at the boundary of the computational domain. Denoting by f_0, g_0, h_0 the numerical values of the perturbation wave amplitudes at the boundary, taken as the line x=0, the C- coefficients satisfy the following system:

$$C_1 + \frac{\beta}{M+1} C_2 - \frac{\beta}{M+1} C_3 = f_0$$

$$-C_1 - \frac{\beta}{1-M} C_2 + \frac{\beta}{1-M} C_3 = g_0$$

(2.10)

$$C_2 + C_3 = h_0$$

The solutions are given as

$$C_1 = \frac{1}{2M} \left[(1+M)f_0 + (1-M)g_0 \right]$$

$$C_2 = \frac{1}{2}\left[h_0 - (f_0 + g_0)\frac{\beta}{2M} \right] \qquad (2.11)$$

$$C_3 = \frac{1}{2}\left[h_0 + (f_0 + g_0)\frac{\beta}{2M} \right]$$

In order to determine the boundary conditions valid at the finite distance location of the boundaries of the computational domain, corresponding to uniform flow conditions at infinity, we have to look at the incoming and outgoing characteristics.

From the properties of the characteristic variables it is known, see for instance Hirsch (1989) for a general presentation, that w'_2 and w'_3 are characteristics propagating from left to right (for positive u), while w'_4 is propagating from right to left for a subsonic flow, since they correspond resp. to wave speeds u, u+c and u-c.

Hence, in order to determine the far field disturbances we have to express that the amplitudes of the incoming characteristic perturbations are zero at infinity, leading to a correction on the physical boundary conditions for finite distances, and that the amplitudes of the outgoing characteristics are defined by the numerical solution at the boundary. These equations are now examined separately for an inlet and an exit boundary.

2.1. Inlet boundary conditions

At an inlet section, w'_2 and w'_3 are incoming characteristics, while w'_4 is propagating from inside the computational domain towards the boundary, for a subsonic inflow, see figure 2.2.

Referring to the solutions (2.1) this implies that the amplitudes h and f must decay to zero for $x \to -\infty$ and consequently, from equation (2.9), that the coefficients C_1 and C_2 have to vanish since they are associated resp. with a constant or an exponentially growing amplitude. Introduced in the relations (2.11), these conditions determine the perturbations f_0 and h_0 in function of g_0, which in turn is obtained from the internal numerical solution.

The following relations are therefore valid at the inlet boundary, instead of $f_0 = h_0 = 0$,

$$f_0 = -\frac{1-M}{1+M}\, g_0$$

$$\qquad (2.12)$$

$$h_0 = \frac{1-M}{\beta}\, g_0 = \frac{\beta}{1+M}\, g_0$$

and the amplitude C_3 of the remaining wave is

$$C_3 = h_0 = \frac{\beta}{1+M}\, g_0 \qquad (2.13)$$

The first order perturbation solution in the region upstream of the inlet boundary is then completely defined for each harmonic as $(x \leq 0)$

$$\left|\begin{array}{c} f \\ g \\ h \end{array}\right| = \frac{g_0\beta}{1+M}\left|\begin{array}{c} \dfrac{-\beta}{M+1} \\ \dfrac{\beta}{1-M} \\ 1 \end{array}\right| e^{\frac{m\pi}{b\,\beta}x} \tag{2.14}$$

The corrected boundary treatment is therefore established as follows. assuming that the incoming flow is isentropic:

i) Develop the numerically computed distribution of the characteristic perturbation

$$w_4' = \frac{p'}{\rho_\infty c_\infty} - q' = \frac{p - p_\infty}{\rho_\infty c_\infty} - (q - q_\infty) \tag{2.15}$$

in a Fourier series in y along the inlet section. With the definitions (1.26) and the first relation (2.12), we have

$$q' = u' = \frac{-1}{1+M_\infty}w_4' = \frac{-1}{1+M_\infty}g_0 \tag{2.16}$$

and hence it is easier to develop the perturbations of the x-component of the velocity in the inlet section, in a cosine-Fourier series

$$u' = \sum_m A_m \cos\frac{m\pi y}{b} \tag{2.17}$$

In practice, 4 to 5 harmonics are sufficient for the required accuracy.

ii) At a duct inlet section, it is customary to fix stagnation pressure and temperature, as well as the inlet flow angle. The present treatment provides a correction to the uniform inlet angle due to the finite distance of the boundary and is defined by applying the A_m-coefficients to the following development, applying equation (2.13),

$$w_2' = v' = q_\infty\theta' = -\beta\sum_m A_m \sin\frac{m\pi y}{b} \tag{2.18}$$

Note the sine-expansion in this formula.

iii) The pressure disturbances at inlet are directly obtained from u' by application of equation (1.31) for isentropic conditions, that is

$$p' = -u'\rho_\infty U_\infty \tag{2.19}$$

without the necessity of performing a Fourier expansion.

In summary, the numerically computed x-component of the velocity perturbations with respect to the far field velocity U_∞ is expanded in a cosine-Fourier series along the inlet section. The resulting Fourier coefficients are applied, after multiplication by $(-\beta)$, as coefficients of a sine-Fourier expansion in order to obtain the flow angle disturbances along the inlet section.

The corrected flow angles are then applied as new boundary conditions.

2.2. Exit boundary conditions

At an exit section, w'_2 and w'_3 are outgoing characteristics, while w'_4 is an incoming characteristic for subsonic exit velocities, figure 2.3. Consequently, only one physical boundary condition can be imposed at a subsonic exit, generally the static pressure.

Referring to the solutions (2.1) this implies that the amplitude g must decay to zero for $x \rightarrow \infty$ and consequently, from equation (2.9), that the coefficient C_3 has to vanish since it is associated with an exponentially growing amplitude. Introduced in the relations (2.11), this condition determines the perturbation g_0 in function of f_0 and h_0, which in turn are obtained from the internal numerical solution.

The following relations are therefore valid at the exit boundary, instead of $g_0 = 0$,

$$g_0 = -\frac{2}{\beta} M h_0 - f_0 \tag{2.20}$$

and the amplitudes of the remaining waves are

$$C_1 = f_0 - \frac{1-M}{\beta} h_0 = f_0 - \frac{\beta}{1+M} h_0$$

$$\tag{2.21}$$

$$C_2 = h_0$$

The first order perturbation solution in the region downstream of the exit boundary is then completely defined for each harmonic as $(x \geq 0)$

$$\begin{vmatrix} f \\ g \\ h \end{vmatrix} = (f_0 - \frac{1-M}{\beta} h_0) \begin{vmatrix} 1 \\ -1 \\ 0 \end{vmatrix} - h_0 \begin{vmatrix} \dfrac{-\beta}{M+1} \\ \dfrac{\beta}{1-M} \\ 1 \end{vmatrix} e^{-\frac{m\pi}{b\beta} x} \tag{2.22}$$

Note that the coefficient C_1 is the amplitude of a constant wave in x and represents a non-decaying contribution, in other words a purely transported quantity. It is shown in the following that the vorticity disturbances are proportional to C_1.

The corrected boundary treatment is therefore established as follows,

i) Develop the numerical distribution of the characteristic perturbations

$$w_2' = v' = q_\infty \theta'$$

$$w_3' = \frac{p'}{\rho_\infty c_\infty} + q' = \frac{p - p_\infty}{\rho_\infty c_\infty} + (q - q_\infty) \qquad (2.23)$$

in a Fourier series in y along the exit section. With the definitions (1.26) and the relations (2.21), the coefficients $[\rho_\infty c_\infty (g+f)/2]$ are equal to the Fourier coefficients B of the expansion of the pressure disturbances in a cosine series and are connected to the v'-expansion by application of equation (2.20). With

$$p' = \sum_m B_m \cos \frac{m\pi y}{b} \qquad (2.24a)$$

$$v' = q_\infty \theta' = \sum_m A_m \sin \frac{m\pi y}{b} \qquad (2.24b)$$

we have,

$$B_m = -\rho_\infty q_\infty \frac{A_m}{\beta} \qquad (2.25)$$

Hence, in order to obtain the pressure corrections due to the finite distance of the exit boundary, it is sufficient to develop only the v'-perturbations in a sine-Fourier series

ii) The corrections to the uniform pressure boundary condition are defined by applying the A_m-coefficients to the following development, leading to the new boundary condition

$$p = p_\infty - \frac{\rho_\infty q_\infty}{\beta} \sum_m A_m \cos \frac{m\pi y}{b} \qquad (2.26)$$

Note the cosine-expansion in this formula.

In summary, the numerically computed y-component of the velocity perturbations is expanded in a sine-Fourier series along the exit section. The resulting Fourier coefficients are applied, after multiplication by the appropriate coefficients, to a cosine-Fourier expansion in order to obtain the new pressure boundary condition.

The solution (2.22) shows that a constant amplitude wave, first term in (2.22), is maintained at downstream infinity. This wave is connected to the C_1 coefficient and is due to the vorticity waves which generate the eigenvalue $\mu_1 = 0$ in equation (2.6). This can also be shown from a direct computation of the vorticity perturbation

$$\omega' = \frac{\partial u'}{\partial y} - \frac{\partial v'}{\partial x} \qquad (2.27)$$

which can be expressed in function of the characteristic variables and the expansions (2.1), for an arbitrary Fourier mode m, by

$$\omega' = -\left(\frac{m\pi}{b}\frac{f-g}{2} + \frac{\partial h}{\partial x}\right)\sin\frac{m\pi y}{b} \tag{2.28}$$

When applying the above relations (2.22), valid at the exit station, we obtain after some algebraic manipulations,

$$\omega' = -\frac{m\pi}{b}C_1\sin\frac{m\pi y}{b} \tag{2.29}$$

This vorticity is generated in the computational domain and is either due to a physical source, such as a non-uniform shock intensity, or to numerical dissipation acting as numerical vorticity sources if the flow is isentropic.

In both cases, the generated vorticity is transported out of the domain, without decaying with downstream distance.

The value of the C_1 coefficient, calculated from the above boundary procedure, is a measure of the numerical accuracy for isentropic flows, since it will be a measure of the numerically generated vorticity.

2.3. Applications: Subsonic channel flow

The treatment of the far field boundary conditions, described above, is applied to a channel flow with subsonic inlet and outlet conditions. The channel is formed by a lower wall with a sinusoidal shape, in order to have a smooth variation of slope, and a rectilinear upper wall.

Calculations are performed in the reference domain, shown in figure 2.4, with 61 points in the streamwise direction and compared to results for a restricted domain of 31 streamwise points, where the boundaries have been taken much closer to the central part of the channel.

The improved boundary treatment is applied to an Euler code developed at the VUB. This code, see Lacor and Hirsch (1988a), (1988b) for a more detailed description, solves the time dependent Euler equations in conservation form on a structured mesh, applying a finite volume, cell-centered discretization. The fluxes are calculated with an upwind method based on flux splitting, extended to second order by variable extrapolation (MUSCL approach) and the TVD property is maintained via the introduction of limiters. The time integration is implicit and the corresponding implicit operators are solved by relaxation methods, coupled to a multigrid technique.

Figure 2.5 shows the isoMach number distribution in the central part of the channel, comparing the results obtained for the extended and restricted domains, the latter with the corrected boundary treatment. Figure 2.5a is obtained with the standard boundary conditions, imposing uniform pressure at exit and zero flow angle at inlet, but only the central part is shown. When the corrected conditions are introduced, figure 2.5b, the computations on the restricted domain become very close to the solution on the extended domain.

Figure 2.6 shows the Mach number distribution on the lower wall, comparing the results obtained for the extended and restricted domains without and with the corrected boundary treatment. Figure 2.6a is obtained with the standard boundary conditions, imposing uniform pressure at exit and zero flow angle at inlet. The errors introduced by these conditions when the limits of the computational domain are too close is clearly seen.

When the corrected conditions are introduced, figure 2.6b, the computations on the restricted domain become very close to the reference solution on the extended domain.

2.3.2. Transonic channel flow

The boundary corrections defined in section 2.2 do not require the flow to be ientropic at outlet, and therefore the method should apply also to non-isentropic conditions, as occurs when a shock appears in the channel. If the inlet Mach number is increased compared to the previous case, a curved shock appears, as seen on figure 2.7, resulting in a non uniform entropy downstream of the shock. Figure 2.7 shows the isoMach number distributions in the central part of the long channel, comparing the results obtained for the extended and restricted domains, the latter with uncorrected (b) and corrected (c) boundary treatment.

The Mach number distributions on the lower and upper walls are shown on figure 2.8, for the three cases of figure 2.7. There is a shift in the shock position by one mesh cell, which is not very significant even on this relatively coarse mesh. The improvement due to the boundary corrections is clearly seen. Another measure of the corrections concerns the inlet angles; the corrected inlet angle for the short channel is 2.6 degrees, to be compared with the value of 2.7 deg. calculated along the same section of the long channel, while in the uncorrected case the inlet angle is fixed at zero degrees. Another display of the effects of the boundary treatment is shown on figure 2.9 where the Mach number profiles are compared at inlet and outlet of the short channel. The differences between the dashed lines and the plus-symbols indicate the amplitude of the corrections on the short channel, while the solid line is the reference value from the long channel. The small difference between the latter and the corrected values of the short channel computation (+ symbols) is probably due to the fact that the boundaries of the long channel have not been taken far enough.

3. FAR FIELD BOUNDARY CONDITIONS FOR CASCADE FLOWS

The method described in section 2 is extended to cascade flows with a geometrical configuration shown in figure 3.1. Cascade flows are characterized by the fact that the passage between two blades is repeated indefinitely in the direction of the cascade front, that is the y-direction, with a periodicity equal to the pitch s (the y-direction corresponds to the tangential, wheel speed, direction in the turbomachine). Due to this periodicity, the computational domain is limited by the blade surfaces and two periodic extensions. At inlet the boundaries AE and BF are periodic, that is all physical flow properties at corresponding points P and P' are identical. Similar properties exist at exit along the segments GC and HD. The inlet and exit sections AB and CD have to be parallel to the cascade front in order to satisfy the periodicity conditions.

The standard physical boundary conditions which are valid strictly at infinity, are uniform values of flow angle, stagnation pressure and temperature at inlet and static pressure at exit.

The objective of the present approach is to define corrections on these conditions due to the finite distance of the limits of the computational domain. Since stationary flows are being considered, stagnation temperature remains constant and hence only the flow angle has to be corrected at inlet and the static pressure at outlet.

The basic equations are given by the linearized system (1.24), written for an arbitrary wave propagation direction $\vec{\kappa}$ and we look for stationary, perturbation solutions of the system (1.24) **in the region between the inlet (or exit) station of the computational domain and the boundary at infinity.**

Since entropy is purely convected and decoupled from the other equations, we can solve separately for the entropy perturbation and remove the corresponding equation from the system (1.24).

Disturbance solutions by separation of variables are sought for the remaining variables in the external region, with a complex Fourier series in y, such as to satisfy periodicity with a period equal to s.

$$w_2' = \sum_{m=1}^{\infty} H_m(x)\, e^{i\frac{2m\pi y}{s}} \tag{3.1a}$$

$$w_3' = \sum_{m=1}^{\infty} F_m(x)\, e^{i\frac{2m\pi y}{s}} \tag{3.1b}$$

$$w_4' = \sum_{m=1}^{\infty} G_m(x)\, e^{i\frac{2m\pi y}{s}} \tag{3.1c}$$

Compared to the duct case, the amplitudes H, F and G are complex quantities, written as

$$H = h_1 - i\, h_2$$
$$F = f_1 - i\, f_2 \tag{3.2}$$
$$G = g_1 - i\, g_2$$

where the subscript m has been removed for clarity of the notations.

The complex form of the solutions (3.1) is a compact way of expressing periodicity, but obviously only the real part has physical significance. The real part of the solution is given, for an arbitrary Fourier mode m, by

$$w_2' = h_1 \cos\phi y + h_2 \sin\phi y$$
$$w_3' = f_1 \cos\phi y + f_2 \sin\phi y \tag{3.3}$$
$$w_4' = g_1 \cos\phi y + g_2 \sin\phi y$$

where the phase angle ϕ is defined by

$$\phi = \frac{2\pi m y}{s} \tag{3.4}$$

Introducing these solutions in the stationary form of equations (1.24) we obtain the following system, for all Fourier modes, as a consequence of the linearity of the perturbation equations, introducing the axial (x) and tangential (y) Mach numbers,

$$M_a = M_\infty \cos\theta_\infty$$

$$M_u = M_\infty \sin\theta_\infty$$

(3.5)

and defining $a = \sin\alpha$ and $b = \cos\alpha$.

$$M_a \frac{\partial H}{\partial x} - \frac{a}{2} \frac{\partial}{\partial x}(F+G) + i\phi M_u H + i\frac{b}{2}\phi(F+G) = 0$$

$$(M_a + b)\frac{\partial F}{\partial x} - a\frac{\partial H}{\partial x} + i\phi bH + i\phi(M_u + a)F = 0$$

(3.6)

$$(M_a - b)\frac{\partial G}{\partial x} - a\frac{\partial H}{\partial x} + i\phi bH + i\phi(M_u - a)F = 0$$

Defining the vector U as

$$U = \begin{vmatrix} H \\ F+G \\ F-G \end{vmatrix}$$

(3.7)

the system (3.6) can be written in matrix form, after some rearrangement,

$$A U_x + B U = 0$$

(3.8)

where the subscript x denotes partial derivative with respect to x and the matrix A is

$$A = \begin{vmatrix} M_a & -\frac{a}{2} & 0 \\ 0 & b & M_a \\ -2a & M_a & b \end{vmatrix} \qquad B = i\phi \begin{vmatrix} M_u & \frac{b}{2} & 0 \\ 0 & a & M_u \\ 2b & M_u & a \end{vmatrix}$$

(3.9)

It is of interest to note at this point that the (F+G) terms are the Fourier coefficients of $2p'/(\rho_\infty c_\infty)$ and that the difference (F-G) represents the expansion of the velocity perturbation along the propagation direction $\vec{\kappa}$, that is $\vec{v}'\cdot\vec{\kappa}$. Note also the appearance of the axial and tangential Mach numbers, which are typical for cascade flows.

Solutions of the form

$$U = U_0 e^{-\mu x}$$

(3.10)

are sought, where μ is equal to the eigenvalues of $(B-A\mu)$, leading to

$$\mu_1 = i\phi\tau \qquad\qquad \text{with} \qquad \tau = \tan\theta_\infty$$

(3.11)

while the two other solutions are obtained from the roots of the quadratic equation, setting $\mu=\phi\lambda$,

$$\lambda^2(1 - M_a^2) + 2i\,\lambda M_a M_u - (1 - M_u^2) = 0 \qquad (3.12)$$

The solutions are

$$\mu_{2,3} = \frac{-i\,\tau M_a M_u \pm \beta}{1 - M_a^2}\,\phi \qquad (3.13)$$

with $\beta^2 = 1 - M^2$, where M is the Mach number of the far field. The appearance of this term indicates that the considered solutions become oscillatory in x at supersonic Mach numbers, since β becomes purely imaginary in this case.

It is of importance to observe that **these eigenvalues are completely independent of the direction** α **of the propagation vector** $\vec{\kappa}$. They depend only on the flow parameters in the far field, namely Mach number and flow angle at infinity. This is to be expected since the linearized solutions of the Euler perturbation equations should have a space dependency based on physical quantities. Only the amplitudes of these waves will be function of the selected propagation direction.

The denominator in equation (3.13) is positive for subsonic axial velocities, which is always the case in practice.

The amplitudes of the solution (3.10) are the eigenvectors of the matrix (B-Aμ), associated to the three eigenvalues (3.11), (3.13). They are easily obtained as

$$U^{(1)} = \begin{vmatrix} \dfrac{1}{2}\dfrac{\xi - \tau}{1 + \xi\tau} \\[2mm] 0 \\[2mm] 1 \end{vmatrix} \qquad U^{(2,3)} = \begin{vmatrix} \dfrac{1}{2}\dfrac{i + \xi\lambda}{i\xi - \lambda} \\[2mm] \dfrac{M_a}{b}\dfrac{\lambda - i\tau}{i\xi - \lambda} \\[2mm] 1 \end{vmatrix} \qquad (3.14)$$

where λ is either of the the the eigenvalues defined by (3.13) and $\xi = \tan\alpha$.

Note that these eigenvectors are independent of the phase angle ϕ, but depend on the propagation direction α. Two of these directions are of interest, the first one corresponds to propagation directions along the free stream at infinity, that is $\alpha = \theta_\infty$ or $\xi = \tau$ and the second one to a propagation along the axial direction, that is $\alpha = 0$. The consequences of these choices are connected to the values of the perturbations to the acoustic waves, as described by the third and fourth characteristics (1.20) and (1.21). In function of the cartesian components u', v' of the velocity disturbances, we have

$$w_3' = \frac{p'}{\rho_\infty c_\infty} + u'\cos\alpha + v'\sin\alpha \qquad (3.15a)$$

$$w_4' = \frac{p'}{\rho_\infty c_\infty} - u'\cos\alpha - v'\sin\alpha \tag{3.15b}$$

and in the first case the velocity disturbances are equal to q', the disturbance of the velocity amplitude, while in the second case, the velocity perturbations are restricted to the axial component.

We will consider in the following the first choice, that is $\alpha = \theta_\infty$ or $\xi = \tau$, observing that

$$\lambda_2 = \frac{1 + i\tau\beta}{i\tau + \beta} \qquad\qquad \lambda_3 = \frac{1 - i\tau\beta}{i\tau - \beta} \tag{3.16}$$

the eigenvectors (3.14) become,

$$U^{(1)} = \begin{vmatrix} 0 \\ 0 \\ 1 \end{vmatrix} \qquad U^{(2)} = \begin{vmatrix} -i\dfrac{\beta}{2} \\ -M \\ 1 \end{vmatrix} \qquad U^{(3)} = \begin{vmatrix} +i\dfrac{\beta}{2} \\ -M \\ 1 \end{vmatrix} \tag{3.17}$$

and the general solution is a linear combination of these eigenvectors

$$U = C_1 \begin{vmatrix} 0 \\ 0 \\ 1 \end{vmatrix} e^{-i\phi\tau x} + C_2 \begin{vmatrix} -i\dfrac{\beta}{2} \\ -M \\ 1 \end{vmatrix} e^{i\phi\tau Kx} e^{-\phi\beta Lx} + C_3 \begin{vmatrix} +i\dfrac{\beta}{2} \\ -M \\ 1 \end{vmatrix} e^{i\phi\tau Kx} e^{\phi\beta Lx} \tag{3.18}$$

with

$$K = \frac{M_a M_u}{1 - M_a^2} \qquad\qquad L = \frac{1}{1 - M_a^2} \tag{3.19}$$

The complex C-coefficients are determined by matching these solutions with the **numerical solution** at the boundary of the computational domain. Denoting by F_0, G_0, H_0 the numerical values of the perturbation wave amplitudes at the boundary, taken as the line x=0, we define real and imaginary parts of the amplitudes

$$H_0 = h_{01} - ih_{02}$$

$$P_0 = F_0 + G_0 = p_{01} - ip_{02} \tag{3.20}$$

$$Q_0 = F_0 - G_0 = q_{01} - iq_{02}$$

The coefficients p_{01} and p_{02} are the Fourier coefficients of the pressure fluctuations, while q_{01} and q_{02} correspond to the expansion of the velocity disturbance q', as can be seen from equations (3.15) above.

The C- coefficients satisfy the following system,

$$\frac{i}{2} \beta (C_3 - C_2) = H_0$$

$$- M (C_2 + C_3) = P_0 \qquad (3.21)$$

$$C_1 + C_2 + C_3 = Q_0$$

Identifying real and imaginary parts and solving for the unknowns leads to the relations for the real values, marked by a superscript (R).

$$2 C_3^{(R)} = -2 \frac{h_{02}}{b} - \frac{p_{01}}{M}$$

$$2 C_2^{(R)} = \quad h_{02} \quad p_{01} \qquad (3.22a)$$

$$M C_1^{(R)} = M q_{01} + p_{01}$$

and for the imaginary components, marked by a superscript (I),

$$2 C_3^{(I)} = -2 \frac{h_{01}}{\beta} + \frac{p_{02}}{M}$$

$$2 C_2^{(I)} = 2 \frac{h_{01}}{\beta} + \frac{p_{02}}{M} \qquad (3.22b)$$

$$M C_1^{(I)} = - M q_{02} - p_{02}$$

Referring to equation (3.3), it is seen that the real parts of P_0 and Q_0 correspond to the coefficients of the cosine terms in the Fourier expansion, while h_{02} is the coefficient of the sine terms in the expansion of w'_2. That is

$$w'_2 = q_\infty \theta' = \sum_m (h_{01} \cos\phi y + h_{02} \sin\phi y)$$

$$(3.23)$$

$$Q = 2q' = \sum_m (q_{01} \cos\phi y + q_{02} \sin\phi y)$$

In order to determine the boundary conditions valid at the finite distance location of the boundaries of the computational domain, corresponding to uniform flow conditions at infinity, we proceed in the same way as in section 2 and express that the amplitudes of the incoming characteristic perturbations are zero at infinity, leading to a correction on the physical boundary conditions for finite distances, and that the amplitudes of the outgoing

characteristics are defined by the numerical solution at the boundary. These equations are now examined separately for an inlet and an exit boundary.

3.1. Inlet boundary conditions

At an inlet section, w'_2 and w'_3 are incoming characteristics, while w'_4 is propagating from inside the computational domain towards the boundary, for a subsonic inflow, see figure 3.2.

Referring to the solutions (3.1) this implies that the amplitudes H and F must decay to zero for $x \to -\infty$ and consequently that the coefficients C_1 and C_2 have to vanish since they are associated resp. with a constant or an exponentially growing amplitude. Introduced in the relations (3.22), these conditions determine the perturbations F_0 and H_0 in function of G_0, which in turn is obtained from the internal numerical solution.

The following relations are therefore valid at the inlet boundary, instead of $F_0 = H_0 = 0$,

$$C_3 = -2i\frac{H_0}{\beta} = -2\frac{h_{02}+ih_{01}}{\beta} = C_3^{(R)} + i\,C_3^{(I)}$$

$$= -\frac{P_0}{M} = Q_0 = q_{01} - iq_{02} = -\frac{p_{01} - ip_{02}}{M}$$

(3.24)

The first order perturbation solution in the region upstream of the inlet boundary is then completely defined for each harmonic as $(x \le 0)$

$$U = (q_{01} - iq_{02})\begin{vmatrix} +i\frac{\beta}{2} \\ -M \\ 1 \end{vmatrix} e^{i\phi\tau Kx}e^{+\phi\beta Lx}$$

(3.25)

The perturbations of the outgoing characteristic w'_4 can be expressed in function of the disturbances of the magnitude of the velocity q' by applying the above relations (3.24), leading to

$$w'_4 = \frac{1}{2}(P - Q) = -\frac{1}{2}(1 + M_\infty)Q = -(1 + M_\infty)q'$$

(3.26)

Therefore, expanding the fourth characteristic is equivalent to a Fourier expansion of the velocity disturbances q'.

The corrected boundary treatment is therefore established as follows, assuming that the incoming flow is isentropic:

i) Develop the numerically computed distribution of the perturbations of the velocity magnitude in the inlet section, in a complete Fourier series

$$q' = \sum_m \left(A_m \cos \phi y + B_m \sin \phi y\right)$$

(3.26)

In practice, 4 to 5 harmonics are sufficient for the required accuracy.

ii) At a cascade inlet section, it is customary to fix stagnation pressure and temperature, as well as the inlet flow angle. The present treatment provides a correction to the uniform inlet angle due to the finite distance of the boundary and is defined by applying the A_m and B_m-coefficients to the following development, applying equation (3.23),

$$q_\infty \theta' = \beta \sum_m \left(B_m \cos \phi y - A_m \sin \phi y \right) \tag{3.27}$$

iii) The pressure disturbances at inlet are directly obtained from q' by application of equation (1.31) for isentropic conditions, that is

$$p' = -q' \rho_\infty q_\infty \tag{3.28}$$

without the necessity of performing a Fourier expansion.

In summary, the numerically computed perturbations of the velocity magnitude are expanded in a complete Fourier series along the inlet section. The resulting Fourier coefficients are applied, after multiplication by β, to a modified Fourier expansion in (3.27) in order to obtain the flow angle disturbances along the inlet section.
The corrected flow angles are then applied as new boundary conditions.

2.2. Exit boundary conditions

At an exit section, w'_2 and w'_3 are outgoing characteristics, while w'_4 is an incoming characteristic for subsonic exit velocities. Consequently, only one physical boundary condition can be imposed at a subsonic exit, generally the static pressure.
Referring to the solutions (3.1) this implies that the amplitude G must decay to zero for

$x \to \infty$ and consequently, from equation (3.1 8), that the coefficient C_3 has to vanish since it is associated with an exponentially growing amplitude. Introduced in the relations (3.21), this condition determines the perturbation G_0 in function of F_0 and H_0, which in turn are obtained from the internal numerical solution.
The following relations are therefore valid at the exit boundary. for the amplitudes of the remaining waves, instead of $G_0 = 0$,

$$C_1 = Q_0 + \frac{P_0}{M}$$

$$C_2 = -\frac{P_0}{M} = \frac{2iH_0}{\beta} \tag{3.29}$$

The first order perturbation solution in the region downstream of the exit boundary is then completely defined for each harmonic as $(x \geq 0)$

$$U = (Q_0 + \frac{P_0}{M}) \begin{vmatrix} 0 \\ 0 \\ 1 \end{vmatrix} e^{-i\phi\tau x} - \frac{P_0}{M} \begin{vmatrix} -i\frac{\beta}{2} \\ -M \\ 1 \end{vmatrix} e^{i\phi\tau Kx} e^{-\phi\beta Lx} \qquad (3.30)$$

Note that the coefficient C_1 is the amplitude of a sinusoidal wave in x and represents a non-decaying contribution, in other words a purely transported quantity. As shown in section 2, the vorticity disturbances are proportional to C_1.

The corrected boundary treatment is therefore established as follows,

i) Develop the numerical distribution of the flow angle perturbations in a Fourier series in y along the exit section.

$$q_\infty \theta' = \sum_m (A_m \cos\phi y + B_m \sin\phi y) \qquad (3.31)$$

With the definitions (3.23) and the relations (3.29) the expansion of the pressure disturbances is directly obtained from

$$P = 2\frac{p'}{\rho_\infty c_\infty} = \sum_m (p_{01} \cos\phi y + p_{02} \sin\phi y) \qquad (3.32)$$

ii) The corrections to the uniform pressure boundary condition are defined by applying the A_m, B_m coefficients to the following development, leading to the new boundary condition

$$p = p_\infty - \frac{\rho_\infty q_\infty}{\beta} \sum_m (B_m \cos\phi y - A_m \sin\phi y) \qquad (3.33)$$

In summary, the numerically computed flow angle perturbations are expanded in a complete Fourier series along the exit section. The resulting Fourier coefficients are applied, after multiplication by the appropriate coefficients, to a Fourier expansion in order to obtain the new pressure boundary condition.

3.3. Applications to cascade flows

The treatment of the far field boundary conditions, described above, is applied to a cascade with subsonic inlet and outlet conditions. The blade is formed by a suction surface with a sinusoidal shape, in order to have a smooth variation of slope, and a rectilinear pressure surface. The shape is identical to the one used in the duct computations of section 2.

Calculations are performed in the reference domain, shown in figure 3.3a with 91 points in the streamwise direction and compared to results for a restricted domain of 55 streamwise points, figure 3.3b, where the boundaries have been taken much closer to the central part of the channel. The blade extends from -0.5 to 0.5 and the long channel extends from -1 to +1; the incidence flow angle is taken equal to 5 degrees.

Figure 3.4 shows the isoMach number distribution in the central part of the channel, comparing the results obtained for the extended and restricted domains, the latter with the corrected boundary treatment. Figure 3.4a is obtained with the standard boundary conditions on the extended computational region, imposing uniform pressure at exit and 5 degrees flow angle at inlet, but only the central part is shown. Figure 3.4b is obtained with the standard boundary conditions on the restricted computational region, imposing the same uniform boundary conditions. When the corrected conditions are introduced, figure 3.4c, the computations on the restricted domain become very close to the solution on the extended domain. This can be noticed in particular by the improved symmetry of the distribution in the second case. Another effect appears on the exit flow angles which is -5.5 for the non-corrected short domain and -5.1 after corrections.

Figure 3.5 shows an enlarged view of the Mach number distribution on the lower (suction side) boundary comparing the results obtained for the extended and restricted domains without and with the corrected boundary treatment. The views cover the region between the leading and trailing edges resp. and the limits of the computational domain. Figure 3.5a shows the inlet region, while figure 3.5b shows the exit region. The solid line is the reference computation with the extended region, the dotted line refers to the short channel and uniform boundary conditions, while the crosses are obtained from the short channel with the corrected boundary treatment. The improvement is clearly seen.

An other illustration of the validity of the theory can be seen from figure 3.6, where the Mach number profiles along the inlet and exit station of the short domains are shown for the same three cases. The improvement is indeed spectacular.

CONCLUSIONS

A method, based on the linearized solutions of the full system of Euler equations has been developed, for channel and cascade flows, in order to correct the uniform boundary conditions, strictly valid at infinity, for the finite distance of the limits of the computational domain. The linearized solutions are obtained by separation of variables with a Fourier expansion in the coordinate along the inlet and exit stations and an exponential variation in the axial direction.

The corrections of the boundary conditions are derived on the basis of characteristic theory, expressing that the incoming characteristic disturbances have to vanish at infinity. The outgoing characteristic disturbances are obtained from a Fourier expansion of the numerical solution at the boundaries. The Fourier coefficients obtained from this expansion are used to generate the non uniform corrections on the physical boundary conditions such as flow angle or pressure.

Computations on duct and cascade flows show the correctness and accuracy of the method, for isentropic and non-isentropic conditions, allowing a considerable reduction of the size of the computational domain.

Some further work should be done to extend the approach to cases where shocks cross the boundaries, in order to cover most of the cases occurring in practice.

ACKNOWLEDGEMENT

REFERENCES

BAYLISS A., TURKEL E. (1982). "Far Field Boundary Conditions for Compressible Flows". Journal Computational Physics, Vol.48, pp.182-199.

HIRSCH Ch., LACOR C., DECONINCK H. (1987). "Convection Algorithms Based on a Diagonalization Procedure for the Multidimensional Euler Equations" Proc. AIAA 8th Computational Fluid Dynamics Conference, AIAA Paper 87-1163, pp.667-676.

HIRSCH Ch. (1988). Numerical Computation of Internal and External Flows, Vol.1: Fundamentals of Numerical Discretization. J. Wiley, London

HIRSCH Ch. (1989). Numerical Computation of Internal and External Flows, Vol.2: Computational Methods for Inviscid and Viscous Flows. J. Wiley, London

LACOR C., HIRSCH Ch. (1988a). " 3D Computations of Complex Flow Systems". Paper presented at the 16th ICAS Conference, Jerusalem.

LACOR C., HIRSCH Ch. (1988b). "Numerical Simulation of the Three-Dimensional Flow around a Butterfly Valve". In Fluid Dynamics in Non-Rotating Turbomachinery Components, ASME Winter Annual Meeting, Proc. FED, Vol. 69, pp.1-12.

ROE P.L. (1986). "Remote Boundary Conditions for Unsteady Multidimensional Aerodynamic Computations". NASA CR-178211, ICASE Report 86-75, NASA Langley Research Center, Hampton, Va.

THOMAS J.L., SALAS M.D. (1986). "Far Field Boundary Conditions for Transonic Lifting Solutions to the Euler Equations". AIAA Journal Vol.24, pp.1074-1080.

VERHOFF, A. (1985). "Modeling of Computational and Solid Surface Boundary Conditions for Fluid Dynamics Calculations". AIAA Paper 85-1496 CP, AIAA 7th Computational Fluid Dynamics Conference.

VERHOFF, A. (1988). "Far Field Computational Boundary Conditions for Internal Flow Problems". Naval Postgraduate School Report, NPS 67-88-001CR, Sept 1988.

VERHOFF A., O'NEIL P.J. (1984). "A Natural Formulation for Numerical Solutions of the Euler Equations". AIAA Paper 84-0163.
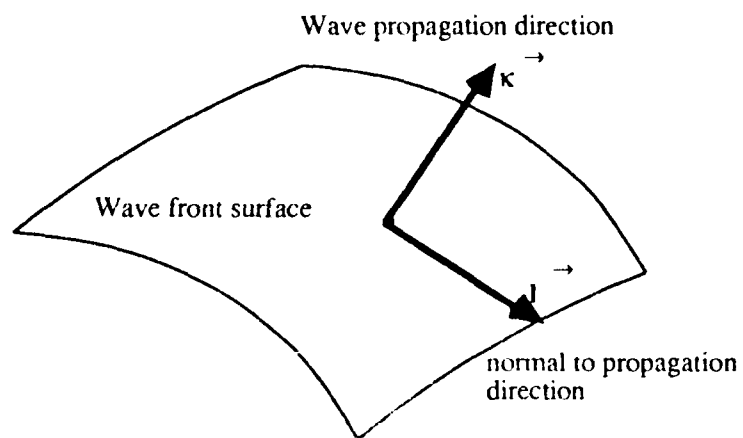
Figure 1.1: Wave front surfaces and wave propagation direction
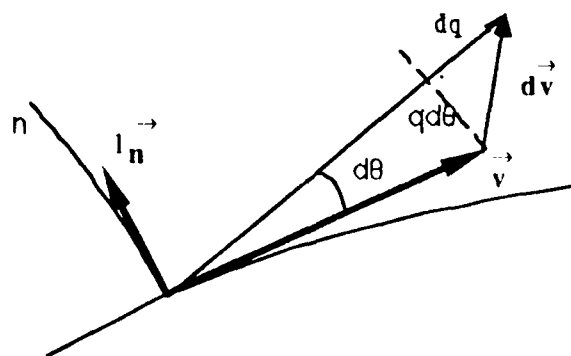
Fig. 1.2: Velocity variations in streamline coordinates
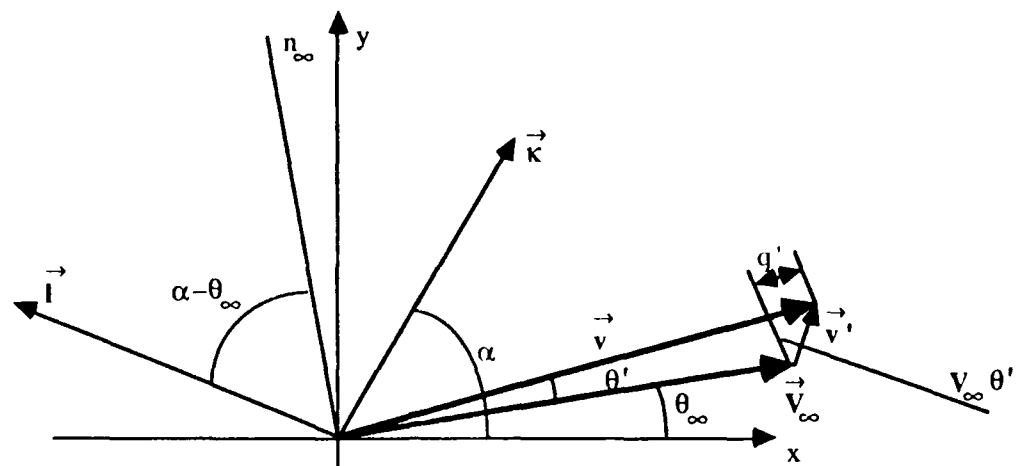
Fig. 1.3: Velocity perturbations and propagation direction
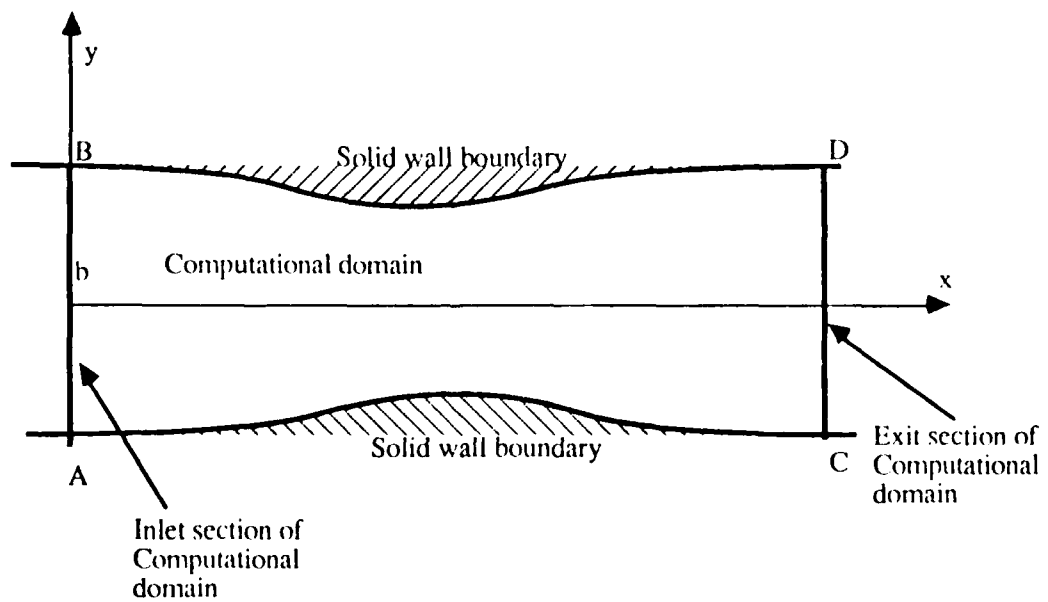
Figure 2.1: Schematic representation of duct geometry
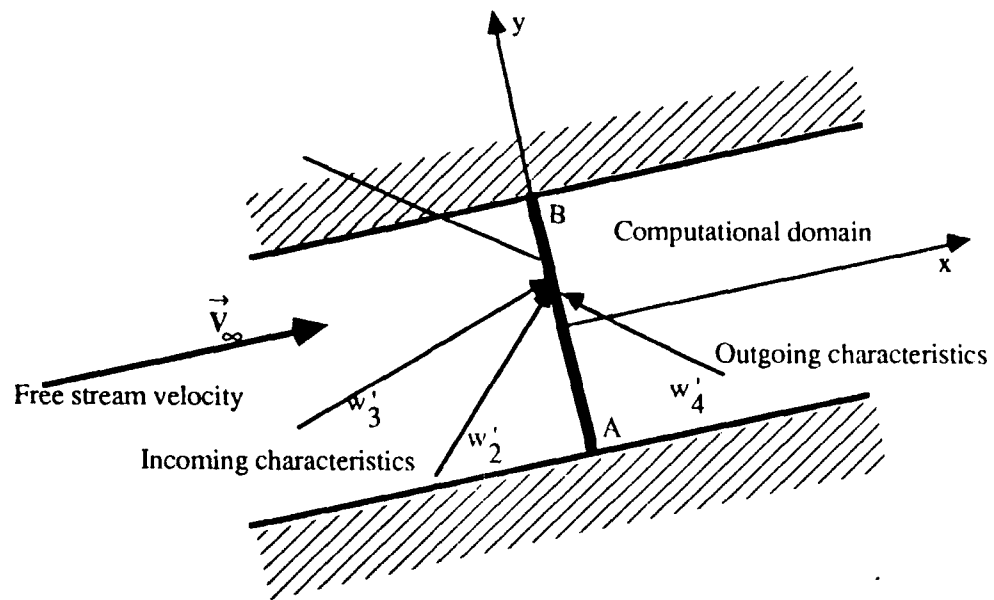
Fig. 2.2: Inlet region and associated characteristics
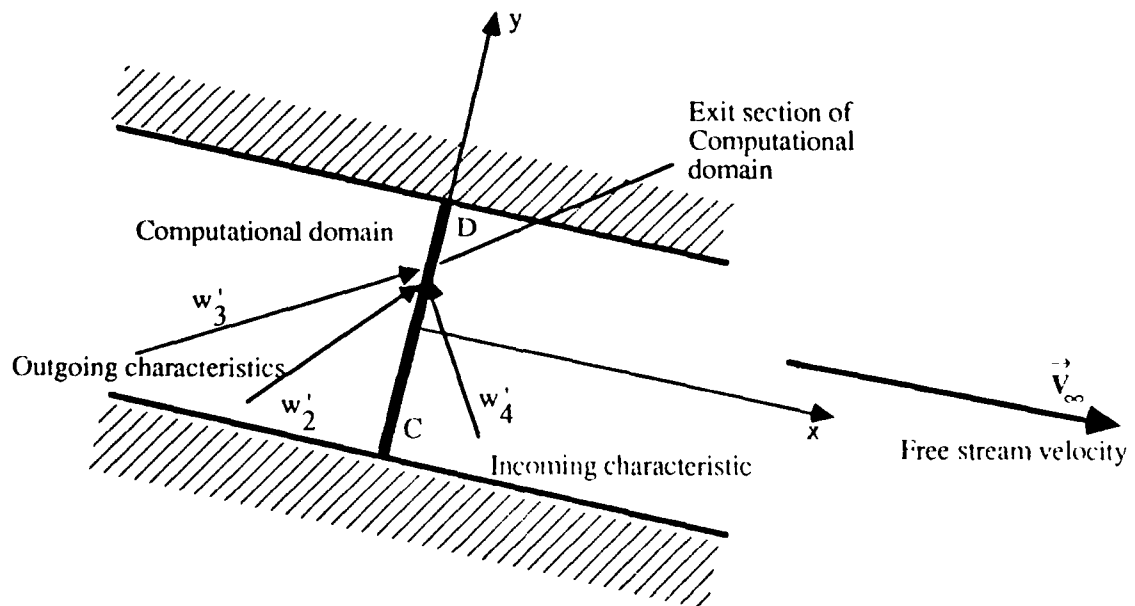
Fig. 2.3:Exit region and associated characteristics
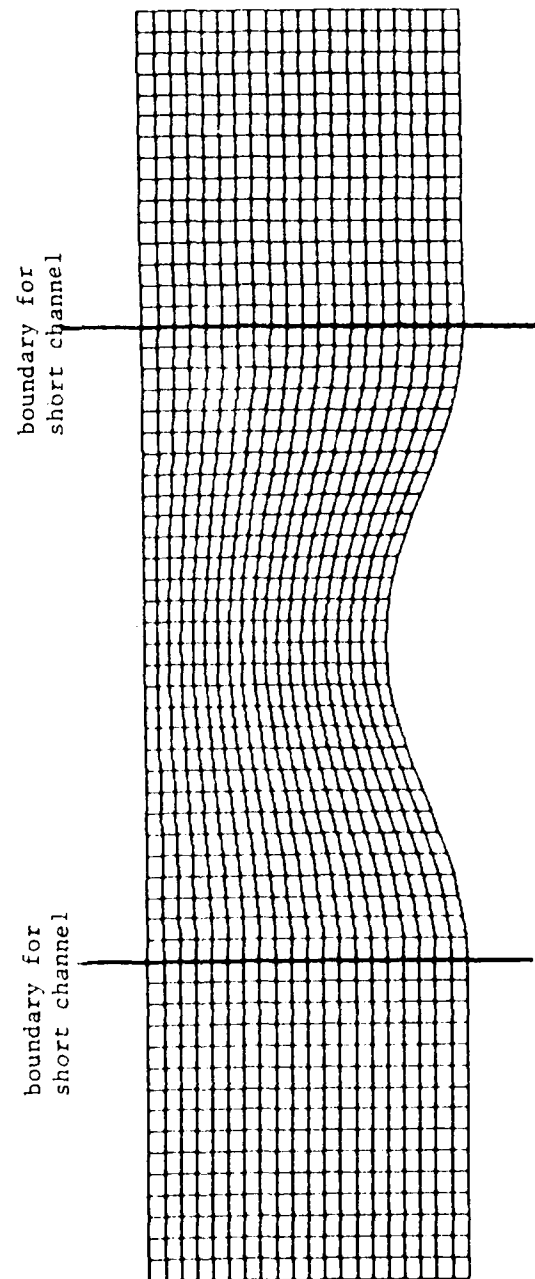
Figure 2.4. : Long (61x21) and short (31x21) mesh for sinusoidal channel

(a)

(b)
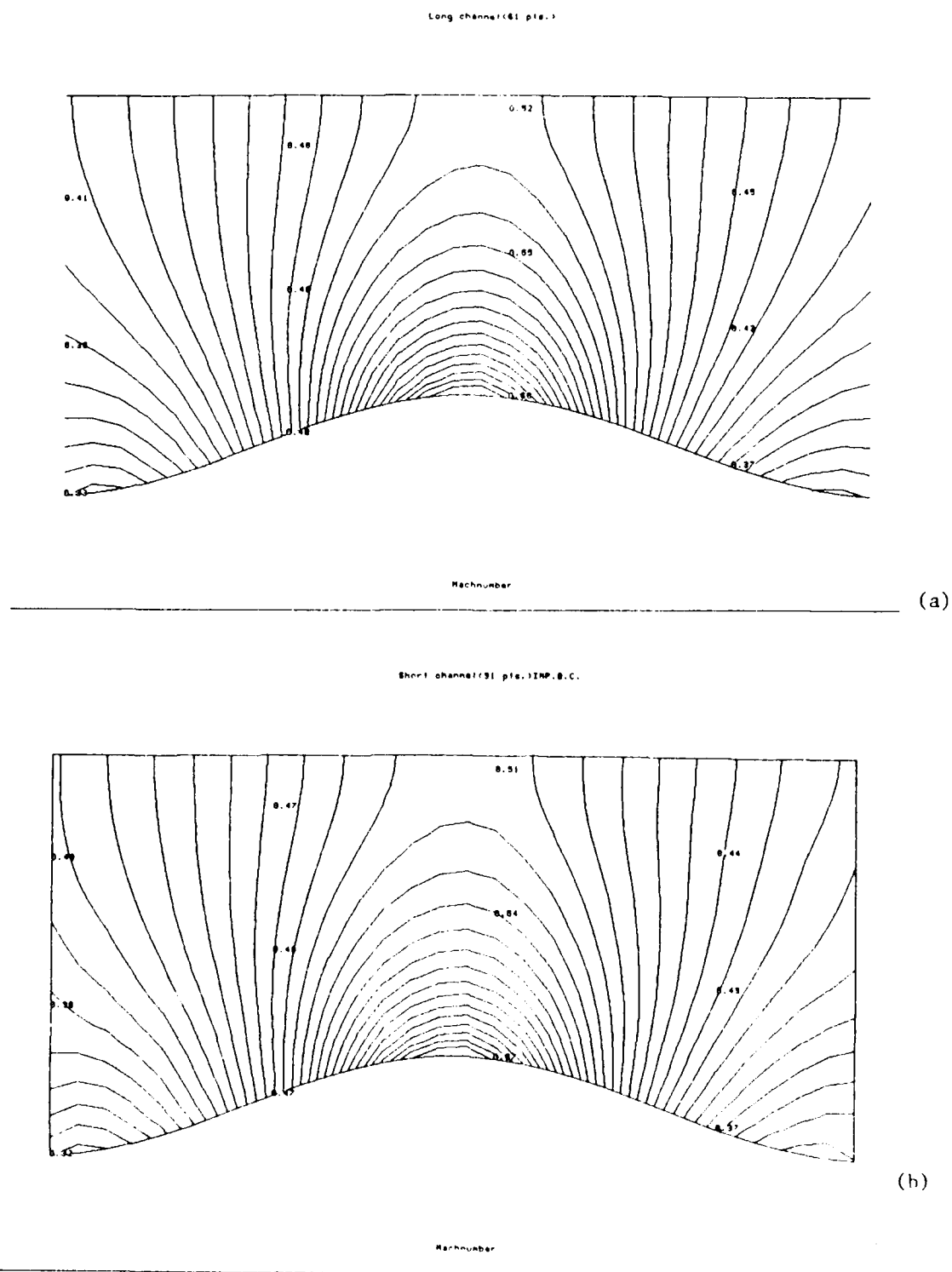
Figure 2.5 : Iso-Mach lines for the central part of the long channel (a) and for the complete short channel (b) with corrected boundary conditions

Dotted = 61 points channel
Solid = 31 points channel

(a)

Dotted = 61 points (no imp.b.c.)
Solid = 31 points (imp.b.c.)

(b)
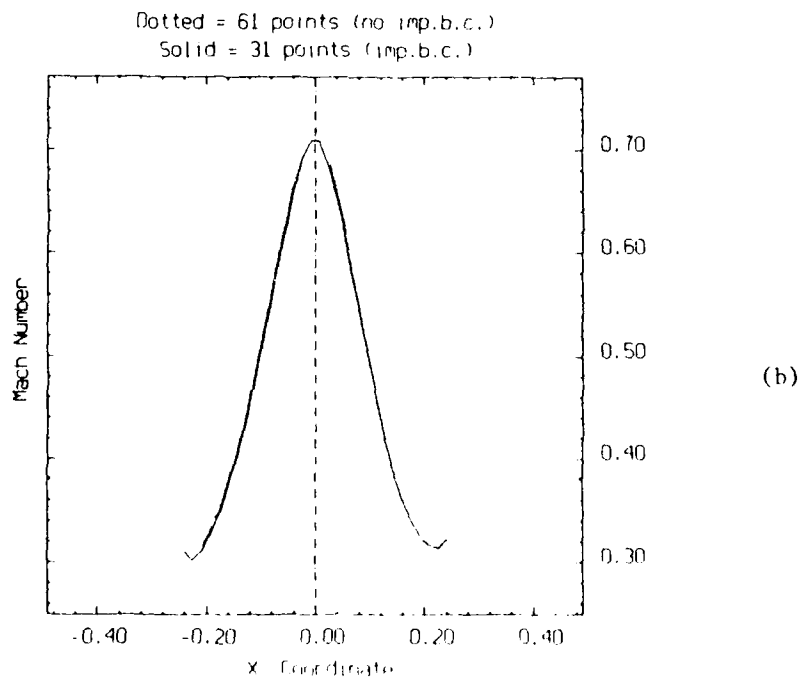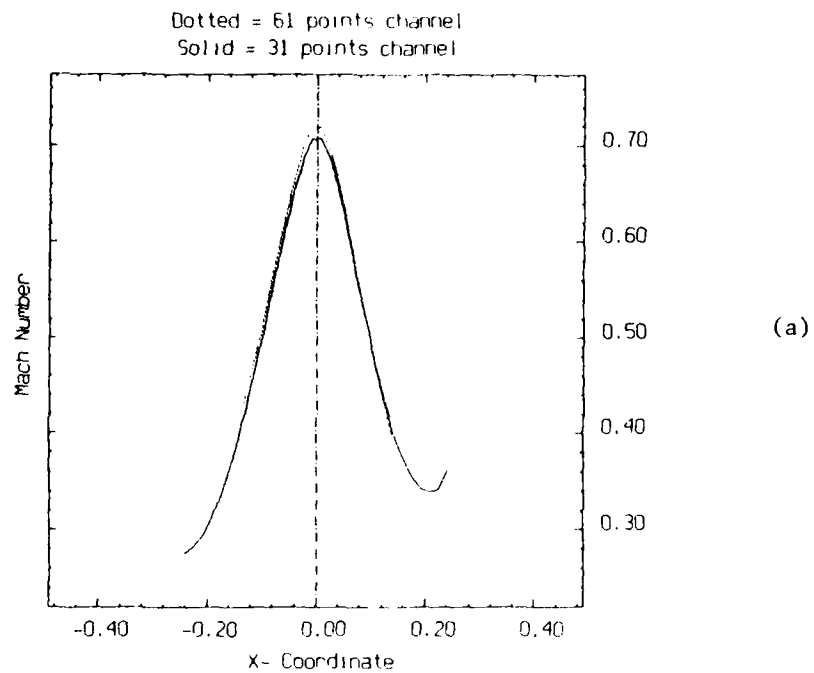
Figure 2.6 : Comparison of Mach number distributions on the lower wall of the
sinusoidal channel :   long channel and
(a) short channel and uncorrected boundary conditions
(b) short channel with corrected boundary conditions

34

Figure 2.7 : Comparison of iso-Mach lines in the central part of the sinusoidal channel at transonic conditions : (a) long channel
(b) short channel and uncorrected boundary conditions
(c) short channel with corrected boundary conditions
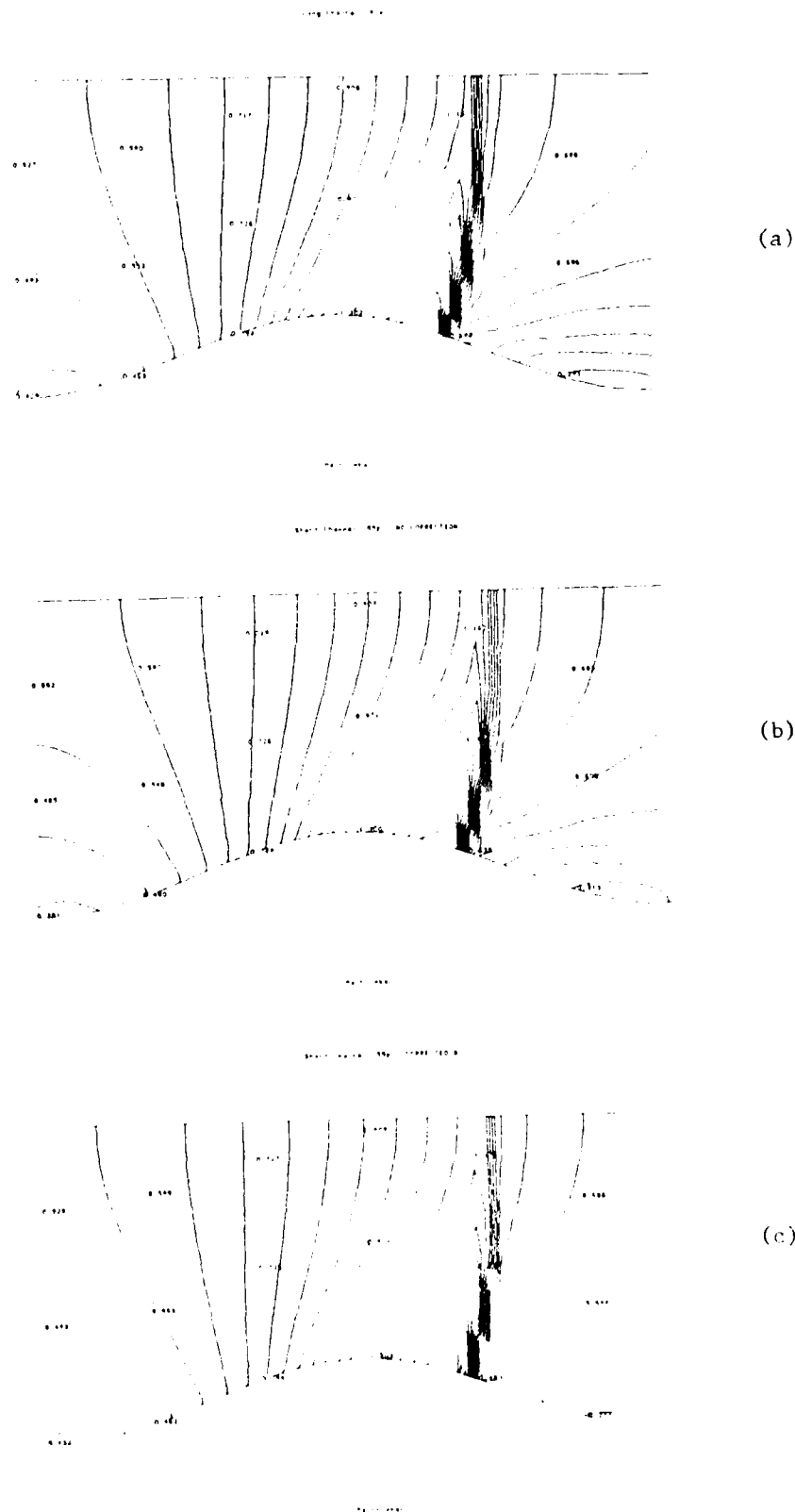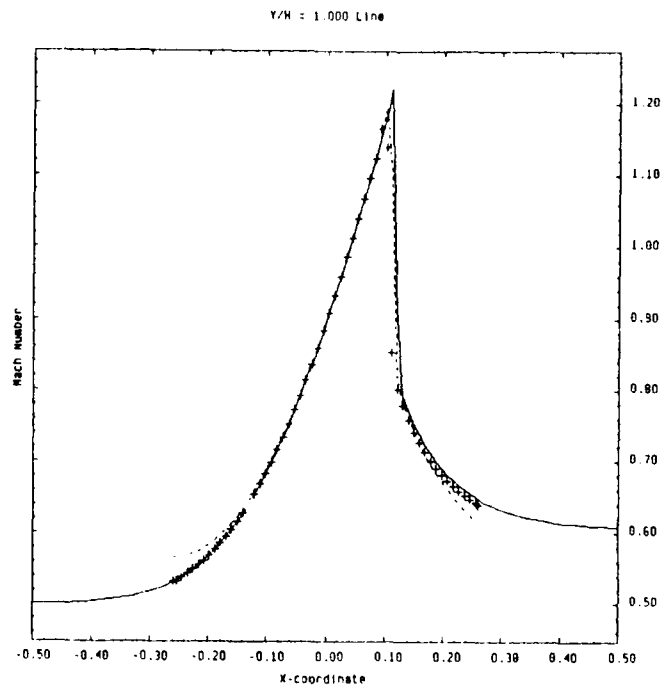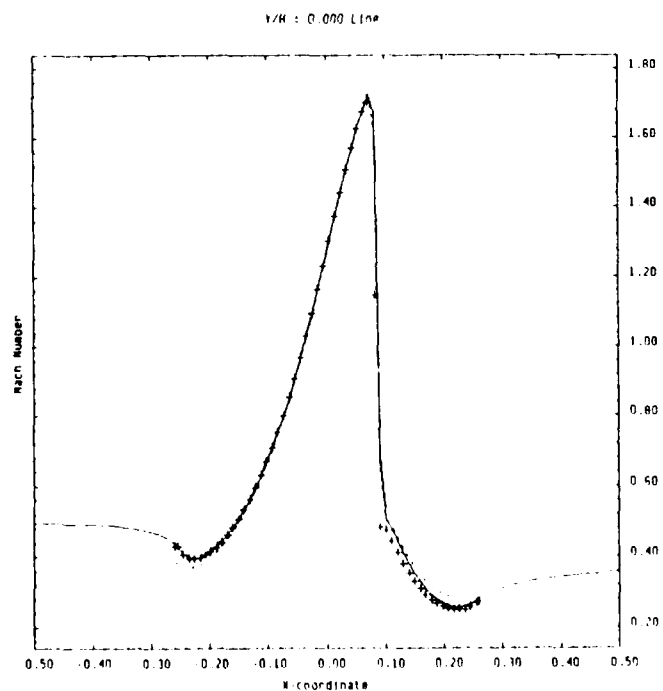
Figure 2.8 : Comparison of Mach number distributions in the central part of the
sinusoidal channel at transonic conditions on lower (a) and upper
(b) walls
Solid line : long channel
Dashed line : short channel and uncorrected boundary conditions
++symbols : short channel with corrected boundary conditions

36

Figure 2.9 : Comparison of Mach number distributions along the inlet (a) and
exit (b) stations of the short sinusoidal channel at transonic
conditions
Solid line : long channel
Dashed line : short channel and uncorrected boundary conditions
++ symbols : short channel with corrected boundary conditions

Fig. 3.1: Cascade geometrical configuration

Fig. 3.2: Cascade inlet flow conditions

Sinus Cascade (Long Mesh)

(a)

1.

0.5

19 cells

52 cells

17 cells

Sinus Cascade (Short Mesh)

(b)

MESH DIMENSION : 55 * 31

4 cells

52 cells

4 cells
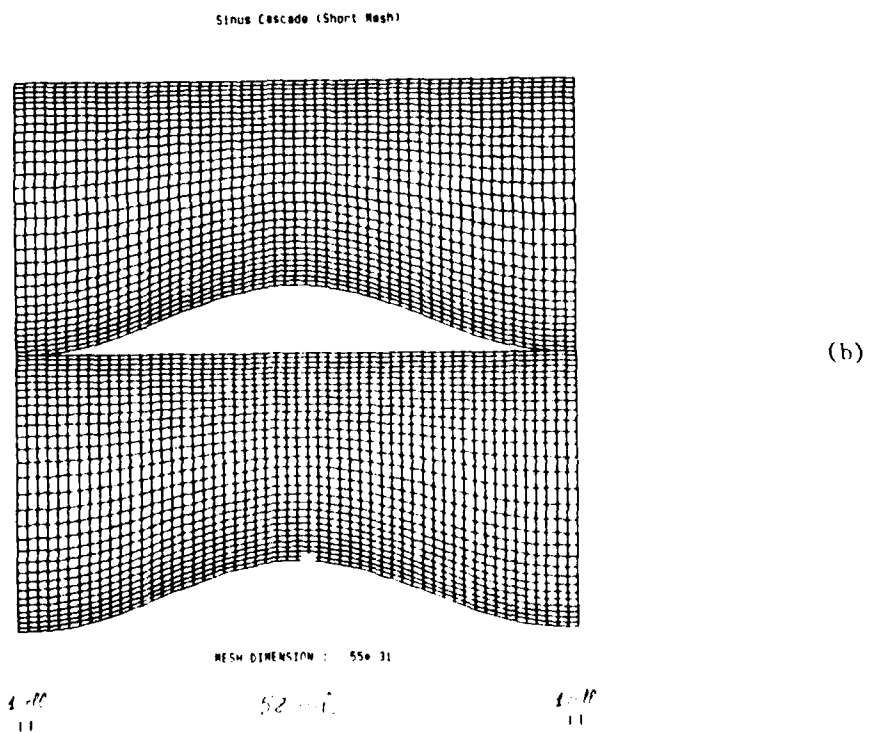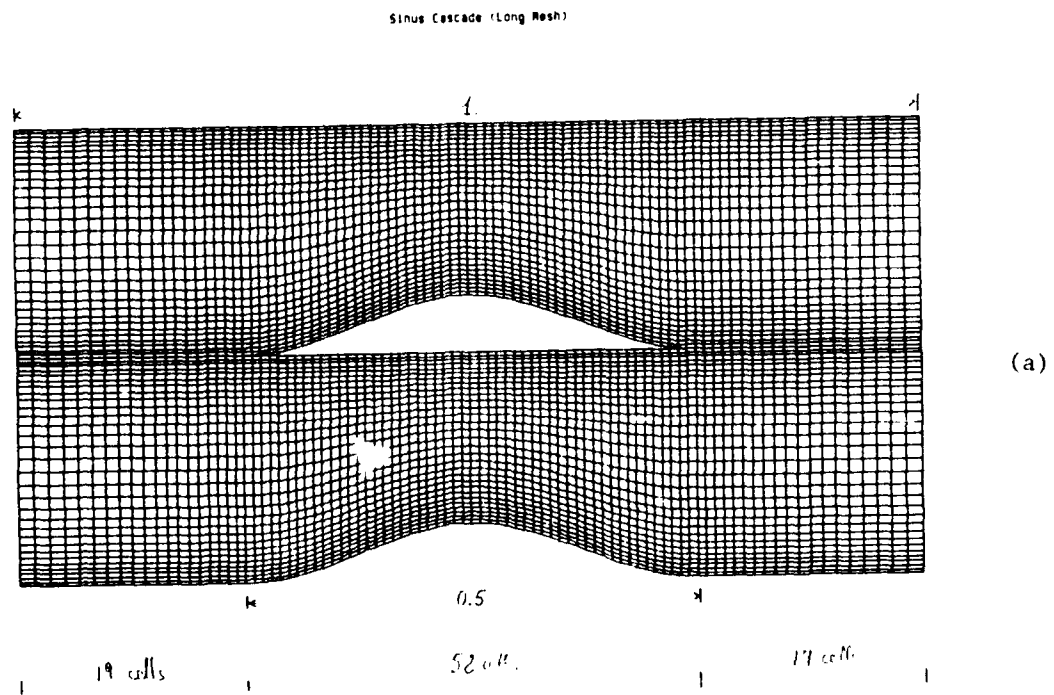
Figure 3.3 : Cascade geometry and mesh for the long and short cascade passages

39
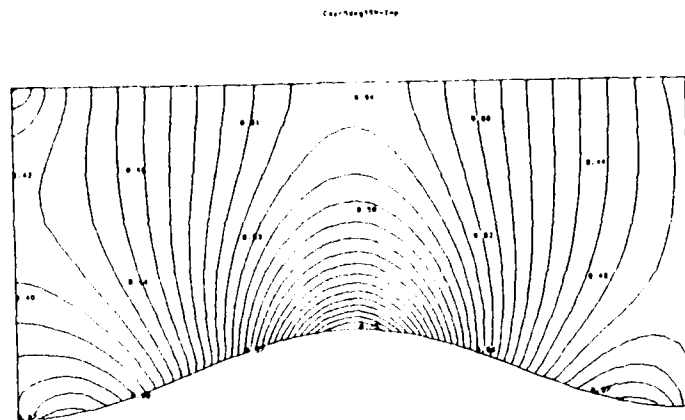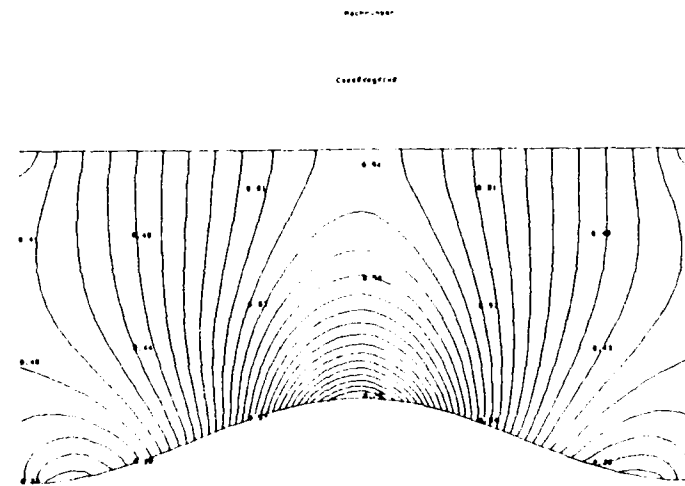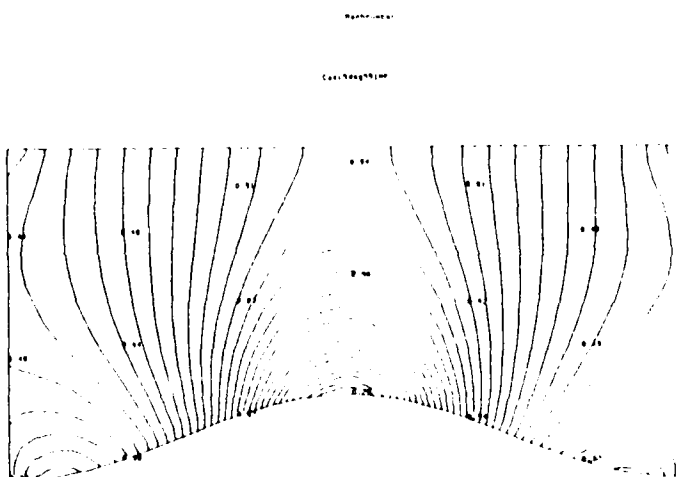
Figure 3.4 : Iso-Mach lines for the central part of the long cascade (a); the
complete short cascade with uncorrected (b) and with corrected (c)
boundary conditions

40
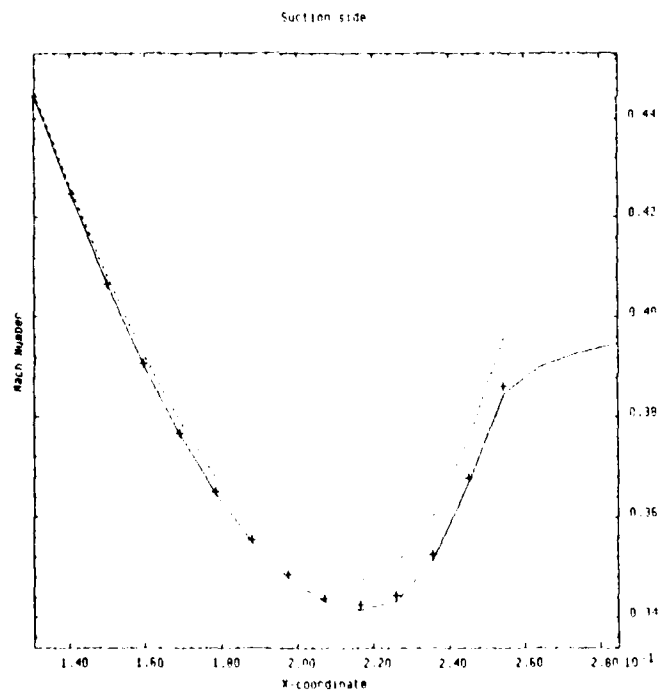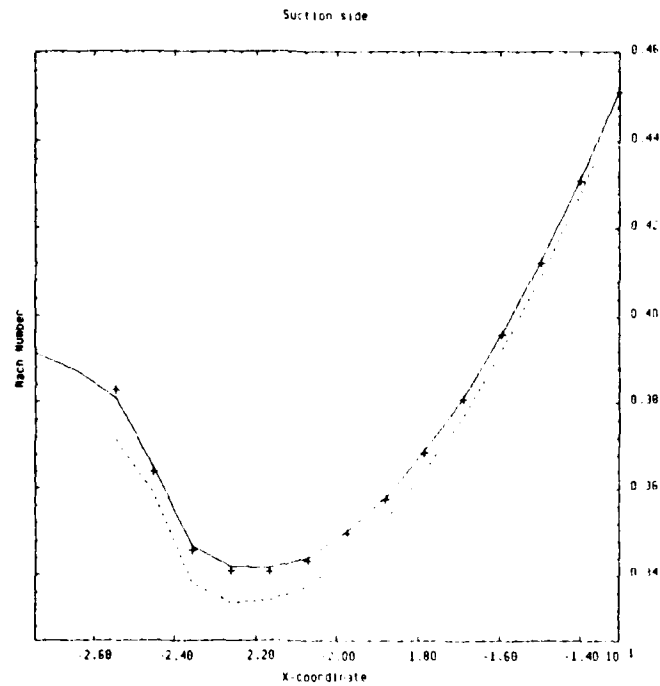
Figure 3.5 : Enlarged view of the Mach number distributions on the suction side
boundary for the three cases of figure 3.4
(a) inlet region between x=0.25 and -0.15
(b) exit region between x=0.15 and 0.25
Solid line : long channel
Dashed line : short channel and uncorrected boundary conditions
++ symbols : short channel with corrected boundary conditions

41
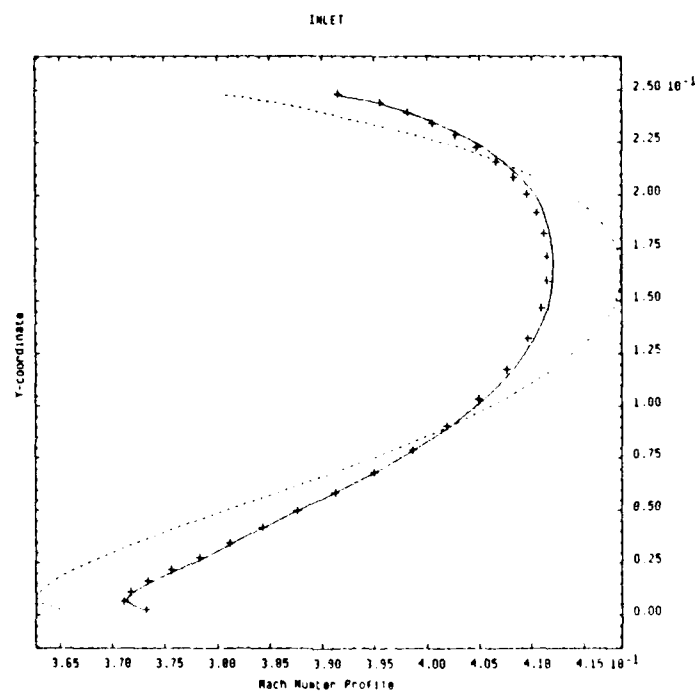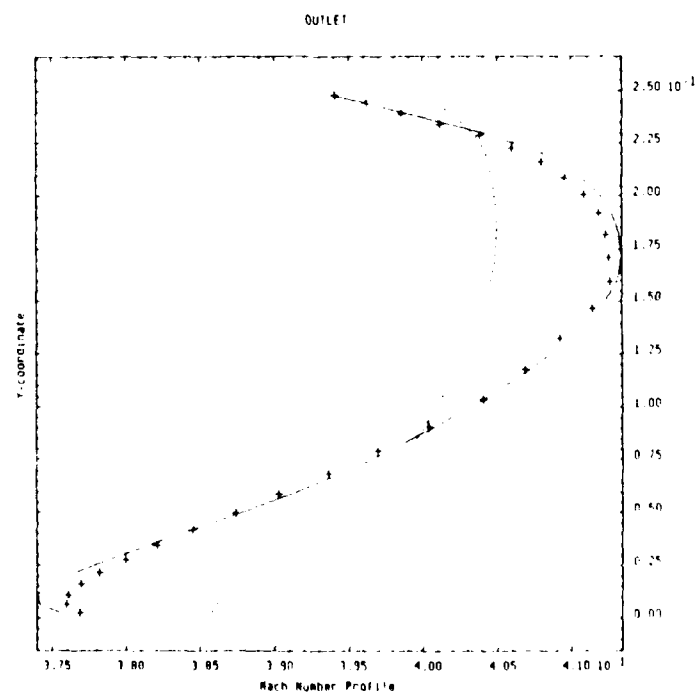
Figure 3.6 : Comparison of Mach number distributions along the inlet (a) and exit (b) stations of the short cascade
Solid line : long channel
Dashed line : short channel and uncorrected boundary conditions
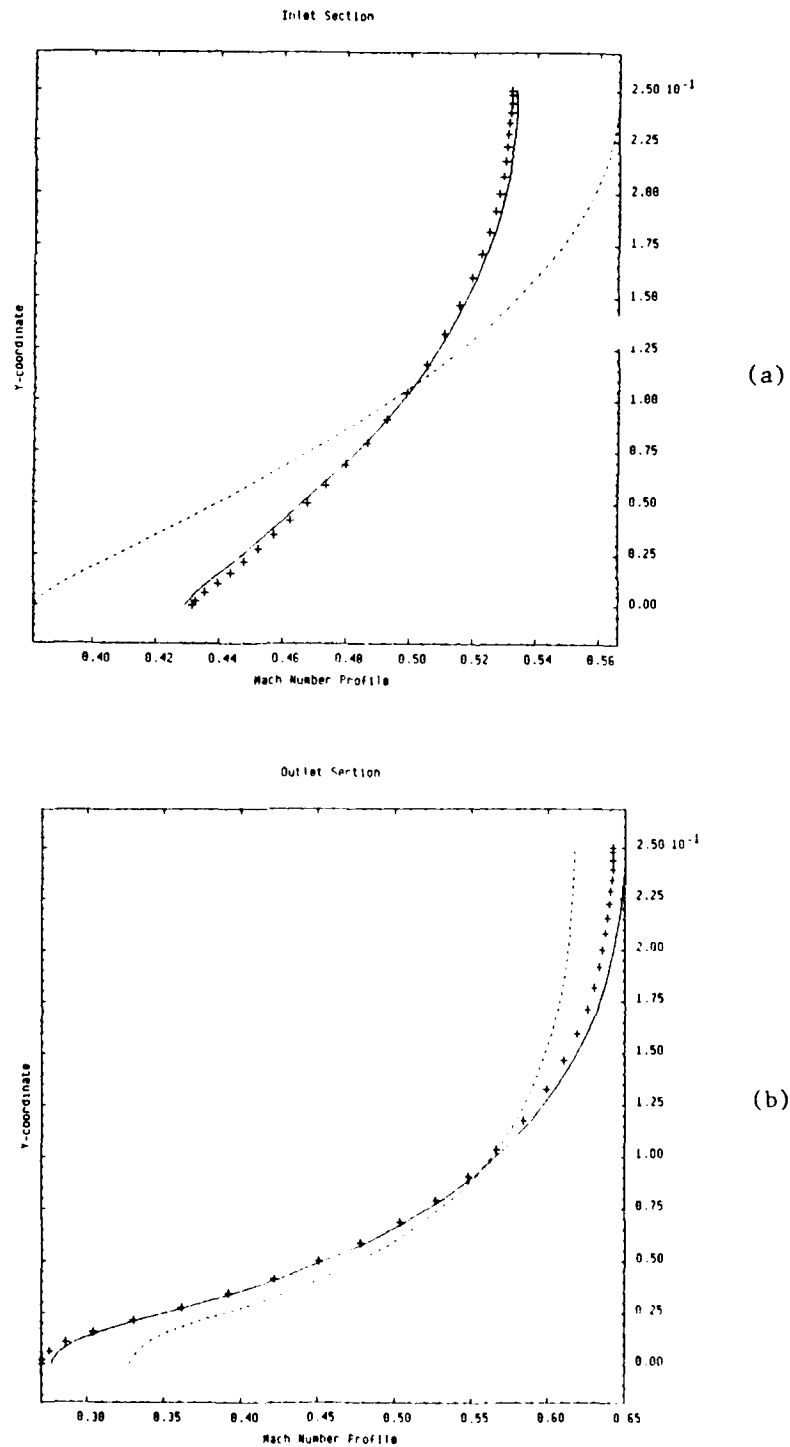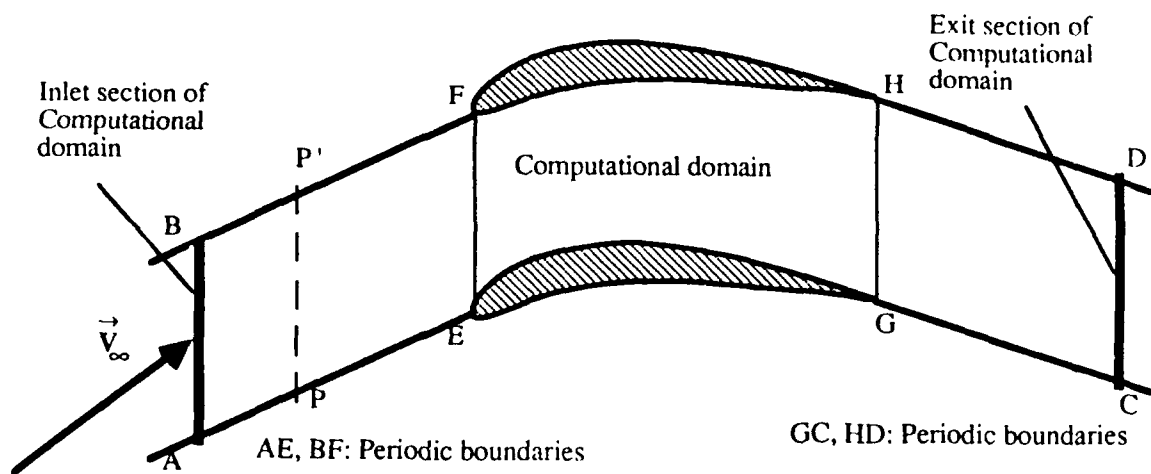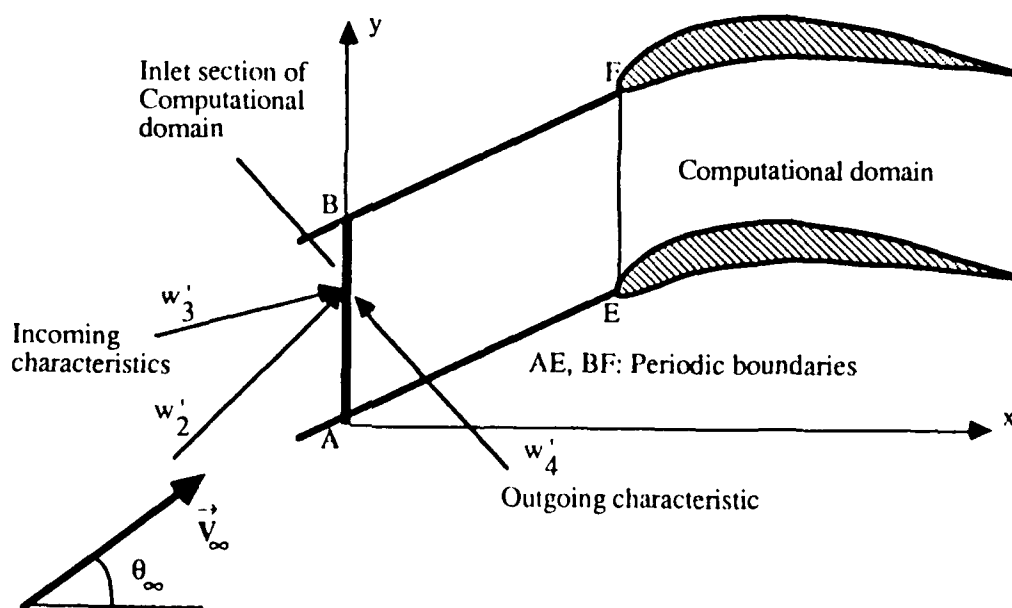++ symbols : short channel with corrected boundary conditions

42

INITIAL DISTRIBUTION LIST

1. Commander
   Naval Air Systems Command
   Washington, DC 20361
   Attention: Code AIR 931   1
               Code AIR 931E   1
               Code AIR 530   1
               Code AIR 536   1
               Code AIR 5004   4
               Code AIR 93D   1

2. Office of Naval Research
   800 N. Quincy Street
   Arlington, VA 22217
   Attention: Dr. Jack Hansen   1

3. Commanding Officer
   Naval Air Propulsion Center
   Trenton, NJ 08628
   Attention: G. Mangano, PE-31   1

4. Commanding Officer   1
   Naval Air Development Center
   Warminster, PA 19112
   Attention: AVTD

5. Library   1
   Army Aviation Material Laboratories
   Department of the Army
   Fort Eustis, VA 23604

6. Dr. Arthur J. Wennerstrom   1
   AFWAL/POTX
   Wright-Patterson AFB
   Dayton, OH 45433

7. Air Force Office of Scientific Research   1
   AFOSR/NA
   Bolling Air Force Base
   Washington, DC 20332
   Attention: Dr. James Wilson

8. National Aeronautics & Space Administration
   Lewis Research Center
   21000 Brookpark Road
   Cleveland, OH 44135
   Attention: Chief, Internal Fluid Mechanics Division   1
               Library   1
               N. Sanger   MS 5-11   1
               J. Adamcyzk   MS 5-11   1
               R. Chima   MS 5-11   1
               P. Sockol   MS 5-11   1
               J. Sanz   MS 5-11   1

43

09. Library   1
    General Electric Company
    Aircraft Engine Technology Division
    DTO Mail Drop H43
    Cincinnati, OH 45215

10. Library   1
    Pratt & Whitney Aircraft Group
    Post Office Box 2691
    West Palm Beach, FL 33402

11. Library   1
    Pratt-Whitney Aircraft Group
    East Hartford, CT 06108

12. Library   1
    Curtis Wright Corporation
    Woodridge, NJ 07075

13. Library   1
    AVCO/Lycoming
    550 S. Main Street
    Stratford, CT 06497

14. Library   1
    Teledyne CAE, Turbine Engines
    1330 Laskey Road
    Toledo, OH 43612

15. Library   1
    Williams International
    P. O. Box 200
    Walled Lake, MI 48088

16. Allison Gas Turbine Division   1
    General Motors Corporation
    P.O. Box 420
    Indianapolis, IN 46206-0420
    Attention: Dr. R.A. Delaney

17. Library   1
    Garrett Turbine Engine Company
    111 S. 34th Street
    P. O. Box 5217
    Phoenix, AZ 85010

18. Professor J. P. Gostelow   1
    School of Mechanical Engineering
    The New South Wales Institute of Technology
    New South Wales
    AUSTRALIA

19. Dr. G. J. Walker   1
    Civil and Mechanical Engineering
       Department
    The University of Tasmania
    Box 252C
    GPO Hobart, Tasmania 7110
    AUSTRALIA

20. Professor F. A. E. Breugelmans   1
    Institut von Karman de la Dynamique
       des Fluides
    72 Chausee de Waterloo
    1640 Rhode-St. Genese
    BELGIUM

21. Professor Ch. Hirsch   30
    Vrije Universiteit Brussel
    Pleinlaan 2
    1050 Brussels
    BELGIUM

22. National Aeronautics & Space Administration
    AMES Research Center
    Moffett Field, CA 94035
    Attention: Dr. Man M. Rai   (RFA:258-D)   1
               Dr. Paul Kutler (RFA:258-D)   1

23. Dr. John Denton   1
    Whittle Laboratory
    Department of Engineering
    Cambridge University
    ENGLAND

24. Library   1
    ONERA
    29, Ave. de la Division Leclerc
    92 Chatillon
    FRANCE

25. Professor D. Adler   1
    Technion Israel Institute of Technology
    Department of Mechanical Engineering
    Haifa 32000
    ISRAEL

26. Dr. P. A. Paranjpe   1
    Head, Propulsion Division
    National Aeronautics Laboratory
    Post Bag 1700
    Bangalore - 17
    INDIA

27. Dr. W. Schlachter   1
    Brown, Boveri Company Ltd.
    Dept. T-T
    P. O. Box CH-5401 Baden
    SWITZERLAND

28. Professor Leonhard Fottner   1
    Department of Aeronautics and Astronautics
    German Armed Forces University
    Hochschule des Bundeswehr
    Werner Heisenbergweg 39
    8014 Neubiberg near Munich
    WEST GERMANY

29. Professor Dr. Ing. Heinz E. Gallus   1
    Lehrstuhl und Institut feur Strahlantiebe
     und Turbourbeitsmashinen
    Rhein.-Westf. Techn. Hochschule Aachen
    Templergraben 55
    5100 Aachen
    WEST GERMANY

30. Dr. Ing. Hans-J. Heinemann   1
    DFVLR-AVA
    Bunsenstrasse 10
    3400 Geottingen
    WEST GERMANY

31. Dr. H. Weyer   1
    DFVLR
    Linder Hohe
    505 Porz-Wahn
    WEST GERMANY

32. United Technologies Research Center
    East Hartford, CT 06108
    Attention: Dr. R.P. Dring   1
               Dr. J. Verdon   1
               Dr. R.L. Davis   1
               Dr. J.E. Carter   1

33. Director, Gas Turbine Laboratory   1
    Aeronautics and Astronautics Department
    31-265 Massachusetts Institute of Technology
    Cambridge, Massachusetts 02139

34. Dr. B. Lakshminaravana   1
    Professor of Aerospace Engineering
    The Pennsylvania State University
    233 Hammond Building
    University Park, Pennsylvania 16802

46

35. Mr. R. A. Langworthy   1
    Army Aviation Material Laboratories
    Department of the Army
    Fort Eustis, VA 23604

36. Mechanical Engineering Department
    Virginia Polytechnic Institute and
       State University
    Blacksburg, VA 24061
    Attention: Professor W. O°Brian   1
                Professor H. Moses   1
                Professor J. Moore   1

37. Professor T. H. Okiishi   1
    Professor of Mechanical Engineering
    208 Mechanical Engineering Building
    Iowa State University
    Ames, Iowa 50011

38. Dr. Fernando Sisto   1
    Professor and Head of Mechanical
       Engineering Department
    Stevens Institute of Technology
    Castle Point
    Hoboken, NJ 07030

39. Dr. Leroy H. Smith, Jr.   1
    Manager, Compressor and Fan
       Technology Operation
    General Electric Company
    Aircraft Engine Technology Division
    DTO Mail Drop H43
    Cincinnati, OH 45215

40. Dr. W. Tabakoff   1
    Professor, Department of Aerospace
       Engineering
    University of Cincinnati
    Cincinnati, OH 45221

41. Mr. P. Tramm   1
    Manager, Research Labs
    Detroit Diesel Allison Division
    Genteral Motors
    P. O. Box 894
    Indianapolis, IN 46206

42. Mr. P. F. Yaggy   1
    Director
    U. S. Army Aeronautical Research Laboratory
    AMES Research Center
    Moffett Field, CA 94035

43. Defense Technical Information Center   2
    Cameron Station
    Alexandria, VA   22314

44. Naval Postgraduate School
    Monterey, CA   93943-5100
    Attention: Professor M. F. Platzer (67P1)   1
               Turbopropulsion Laboratory (67Sf) 15
               Library (1424)   2
               Research administration (012)   1

45. Dr. August Verhoff   1
    McDonnell Aircraft Company
    Mail Code: 341/32/2/MS122
    P.O. Box 516
    St. Louis, MO 63166

46. Dr. Steven Shamroth   1
    Scientific Research Associates
    P.O. Box 498
    Glastonbury, CT 06033

47. Dr. Chunill Hah   1
    General Electric Company
    CR & D K-1
    Schenectady, NY 12345